Published in final edited form as:

Traffic. 2016 March ; 17(3): 191–210. doi:10.1111/tra.12356.

Analysis of COPII vesicles indicates a role for the Emp47-Ssp120 complex in transport of cell surface glycoproteins

Neil G. Margulis[1], **Joshua D. Wilson**[1], **Christine M. Bentivoglio**[1], **Nripesh Dhungel**[2,3], **Aaron D. Gitler**[2], and **Charles Barlowe**[1,*]

[1]Department of Biochemistry, Geisel School of Medicine at Dartmouth, Hanover, NH 03755 USA

[2]Department of Genetics, Stanford University School of Medicine, Stanford, CA 94305 USA

Abstract

Coat protein complex II (COPII) vesicle formation at the endoplasmic reticulum (ER) transports nascent secretory proteins forward to the Golgi complex. To further define the machinery that packages secretory cargo and targets vesicles to Golgi membranes, we performed a comprehensive proteomic analysis of purified COPII vesicles. In addition to previously known proteins, we identified new vesicle proteins including Coy1, Sly41 and Ssp120, which were efficiently packaged into COPII vesicles for trafficking between the ER and Golgi compartments. Further characterization of the putative calcium-binding Ssp120 protein revealed a tight association with Emp47 and in *emp47*Δ cells Ssp120 was mislocalized and secreted. Genetic analyses demonstrated that *EMP47* and *SSP120* display identical synthetic positive interactions with *IRE1* and synthetic negative interactions with genes involved in cell wall assembly. Our findings support a model in which the Emp47-Ssp120 complex functions in transport of plasma membrane glycoproteins through the early secretory pathway.

Keywords

Endoplasmic reticulum; Golgi; COPII coat; vesicle budding; protein trafficking; protein secretion; cargo receptors

The biogenesis of secretory proteins is initiated at the endoplasmic reticulum (ER) where nascent polypeptides are translocated across the ER membrane and folded into transport competent forms. For anterograde transport from the ER, fully folded secretory cargos are then packaged into COPII (coat protein complex II) coated transport intermediates for delivery to the Golgi complex (1). Selective export of cargo from the ER is directed by the inner layer Sec23/24 adaptor subunits of COPII, which form ternary cargo complexes with the Sar1 GTPase and segregate anterograde cargo from ER resident proteins (2, 3) at specific ER exit sites (4–6). Polymerization of outer layer Sec13/31 subunits at ER exit sites produces cage-like structures that drive membrane deformation and produce transport

*Corresponding author: Charles.Barlowe@Dartmouth.Edu.
[3]Present address: Singer Instruments, Roadwater, Watchet, Somerset TA23 0RE UK

Supporting Information

Additional Supporting Information may be found in the online version of this article.

carriers (7, 8). In addition to nascent secretory cargo, the COPII machinery selectively incorporates vesicle components that are required for targeted membrane fusion and bi-directional transport between the ER and Golgi compartments (9).

To efficiently export a diverse array of secretory proteins from the ER, additional transmembrane receptor proteins act in concert with the COPII machinery to chaperone and/or link cargo to COPII adaptor subunits (10). A well-characterized example is the mammalian lectin-binding ERGIC-53/LMAN1 (henceforth ERGIC53) cargo receptor that is required for efficient transport of coagulation factors V and VIII, specific cathepsins and additional glycoprotein cargo (11–13). Other examples include p24 protein packaging of GPI-anchored cargo (14), Erv29 incorporation of soluble secretory cargo (15) and Erv14-dependent export of specific transmembrane cargo (16, 17). However, the mechanisms by which receptors act to capture the full range of diverse cargo, how cargo binding is regulated and how export is coordinated with the ER quality control machinery are open questions in the trafficking field.

Proteomic analyses of isolated intermediates in the early secretory pathway have proven valuable in defining cargo sorting and vesicle fusion machineries (18–20). In this study we apply a comprehensive proteomic approach to identify additional factors that are efficiently packaged into yeast COPII vesicles and appear to cycle between the ER and Golgi compartments. The putative Ca^{2+} binding protein Ssp120 was detected as an abundant COPII vesicle cargo and further analyses indicated this protein forms a tight complex with Emp47, a putative cargo receptor in yeast that shares amino acid identity and structural similarity to the mammalian carbohydrate-binding cargo receptor ERGIC53 (21–23). Recent large-scale surveys also identified and partially characterized the Emp47-Ssp120 interaction (17, 24). In accord with these findings we observed that Ssp120 depends on Emp47 for efficient incorporation into COPII vesicles and a normal distribution between ER and Golgi compartments. Our results indicate that the Emp47-Ssp120 complex acts together to manage secretory cargo transport through the early secretory pathway.

Results

Identification of COPII vesicle proteins through *en bloc* mass spectrometry analysis

A protocol to generate ER-derived vesicles *in vitro* using washed microsomes and purified COPII components was scaled up for purification and detection of vesicle polypeptides on protein-stained SDS-PAGE gels (19, 25, 26). As shown in Figure 1A, silver staining revealed increased levels of a number of protein species coincident with the addition of COPII components. To analyze vesicle polypeptide content, samples were concentrated and run partially into an SDS-PAGE gel. After staining with colloidal Coomassie, each lane was cut into three sections as depicted in Figure 1B, which were then submitted for protein analyses by microcapillary LC/MS/MS. Gel sections were cut unevenly to compensate for the higher concentration of proteins near the dye front.

Analysis by mass spectrometry yielded peptide identification of 290 unique proteins across the six panels (Table S1). Of these identified proteins, 152 had peptide representatives in both mock (no added COPII components) and plus COPII-component samples. Importantly,

the number of unique peptides identified for known ER vesicle proteins was greater in the plus COPII-component sample compared to the mock control. We used this comparison to qualitatively assess COPII-dependent protein enrichment. Table 1 reports the peptide representation of previously documented ER vesicle proteins, representative secretory cargo proteins, and candidate vesicle proteins, which displayed ER vesicle-like peptide representation. The list of known vesicle proteins identified here includes most we had identified previously (19) as well as several other notable Erv proteins described elsewhere (27–31). This indicates the *en bloc* method is robust and should assist in identification of new ER vesicle proteins.

The three proteins with ER vesicle-like peptide representation (Coy1, Sly41, and Ssp120) are non-essential and thought to function in the early secretory pathway, but have not been localized to ER-derived vesicles before. Peptides from Coy1 (CASP Of Yeast) correspond to the ORF YKL179c that encodes an ≈80 kDa single pass type II transmembrane protein containing extensive cytoplasmic coiled-coil regions, and shares structural and sequence similarity with the mammalian family of Golgin proteins. Coy1 localizes to the early Golgi compartments at steady-state and deletion of *COY1* was shown to alleviate growth defects displayed by cells harboring deletions of the genes encoding the SNARE proteins Gos1 and Sec22, which are involved in ER-Golgi transport (32). Peptides from Sly41 (Suppressor of Loss of *YPT1*) correspond to the ORF YOR307c that encodes a ≈51 kDa multipass membrane protein with sequence similarity to solute transporters (33–35). Sly41 localizes to the ER at steady-state, and multi-copy expression of *SLY41* was shown to suppress the loss of *YPT1*, an essential Rab GTPase required for ER-Golgi transport. Peptides from Ssp120 (*S. cerevisiae* Secretory Protein) correspond to the ORF YLR250w that encodes a ≈27 kDa soluble protein containing an *N*-terminal signal sequence and dual calcium-binding EF-hand motifs (35–37). Ssp120 localizes to Golgi compartments and shares structural and sequence similarity with the Golgi-localized mammalian nucleobindins (38, 39).

Efficient packaging of newly identified ER vesicle proteins into COPII vesicles *in vitro*

The initial requirement of an authentic ER vesicle protein is selective export from ER membranes under conditions that reconstitute COPII vesicle budding (16, 19). To confirm the selective packaging of ER vesicle proteins identified by mass spectrometry, we first created strains with a C-terminal triple HA-epitope tag at the chromosomal locus of the genes encoding each of these proteins (40). Washed semi-intact cells prepared from untagged wild-type, *COY1-HA*, *SLY41-HA*, and *SSP120-HA* strains were used to perform reconstituted *in vitro* vesicle budding assays (Figure 2A). Relative packaging efficiencies were assessed in immunoblots by comparing the level of specific proteins packaged into vesicles synthesized in the presence or absence of purified COPII proteins with total lanes containing 10% of the total reactions (19). Coy1-HA (17%), Sly41-HA (33%), and Ssp120-HA (13%) were efficiently incorporated into COPII vesicles at levels comparable to the positive control Erv29 (25%, 30% and 21%, respectively), whereas the ER resident Sec61 (negative control) was not efficiently packaged. Therefore, we observed that Coy1, Sly41, and Ssp120 fulfill the initial requirement for authentic ER vesicle proteins.

For the remainder of this report, we chose to further characterize the role of Ssp120 in the early secretory pathway. Further analysis of Coy1 and Sly41 will be described elsewhere. We next generated a polyclonal antibody against Ssp120 to determine the packaging efficiency of the endogenous form. Immunoblot of the wild-type and *SSP120-HA* budding assay samples above with the polyclonal anti-Ssp120 antibody showed native Ssp120 and Ssp120-HA were incorporated into COPII vesicles at similar levels (14% and 13%, respectively), indicating that the epitope tag does not affect ER packaging of Ssp120 (Figure 2C, blot labeled α-Ssp120). Next, we performed *in vitro* budding assays on microsomes prepared from wild-type and *ssp120*Δ strains (Figure 2D). Ssp120 was efficiently packaged (15%) in the wild-type strain as in Figure 2C, while the absence of an immunoreactive band in the *ssp120*Δ strain demonstrates specificity of the anti-Ssp120 antibody. Both strains displayed similar levels of Erv29 incorporation into COPII vesicles (18% for wild-type and 19% for *ssp120*Δ) and exclusion of Sec61, indicating that the *ssp120*Δ deletion does not generally affect the level of COPII vesicle budding or protein sorting at the ER. We confirmed that ER to Golgi transport is normal in *ssp120*Δ strains using a more sensitive *in vitro* transport assay that monitors the vesicle budding, tethering, and fusion stages (Figure S1) (41, 42). Consistent with our observations, previous work found the *ssp120*Δ mutation did not interfere with secretion, glycosylation, or enzymatic activity of the secreted acid phosphatase Pho5 (36). These results suggest that Ssp120 traffics between ER and Golgi compartments, but is not required for ER to Golgi transport in general.

Emp47 co-immunoprecipitates with Ssp120

Many ER vesicle proteins contain cytosolic sorting signals that bind directly to cytosolic COPI and COPII coat complexes for efficient vesicle packaging (10). However, Ssp120 cannot access these coat complexes because it is confined to the lumen and lacks known vesicle trafficking signals (e.g., the HDEL ER retrieval motif). Thus, we reasoned that selective COPII-vesicle packaging and steady-state Golgi localization of Ssp120 could be explained by association with a transmembrane ER vesicle protein. To test this, we performed native immunoprecipitation experiments to identify Ssp120-interacting proteins. Budding competent microsomes prepared from wild-type and *SSP120-HA* strains were solubilized in Triton X-100 and immunoprecipitated with monoclonal anti-HA antibodies. A protein of ~47 kDa was co-precipitated at near-stoichiometric levels with Ssp120-HA, but was not detected in the untagged wild-type strain (Figure 3A). This band was excised and identified as Emp47 by mass spectrometry. The co-immunoprecipitation of Emp47 with Ssp120-HA was confirmed by immunoblot with polyclonal anti-Emp47 antibodies (Figure 3B). As a control, the soluble protein CPY was not immunoprecipitated, indicating specificity of the Ssp120-Emp47 interaction. To rule out any potential influences of the HA-epitope tag, the immunoprecipitation was repeated using polyclonal anti-Ssp120 antibodies on solubilized microsomes from wild-type and *ssp120*Δ strains. As shown in Figure 3C, similar levels of Emp47 co-precipitated with endogenous Ssp120 as with Ssp120-HA.

Emp47 is a non-essential, single pass type I transmembrane protein with a larger *N*-terminal lumenal portion that contains the carbohydrate recognition domain (21, 23). The *C*-terminal cytoplasmic tail sequence of Emp47 contains COPI and COPII sorting signals that cycle the protein between ER and Golgi compartments with a predominant localization to the early

Golgi under steady-state conditions (19, 21, 22). Emp47 is thought to function in sorting a subset of glycoproteins into COPII vesicles for export from the ER (21, 22) and the protein assembles into homo-oligomers as well as heter-oligomers with its paralog Emp46 (43). Additional Ssp120-HA immunoprecipitation experiments revealed co-precipitation of Emp46, but the interaction between Emp47 and Ssp120-HA was not affected in *emp46*Δ cells (Figure S2). Moreover both Emp47 and Ssp120 are efficiently packaged into COPII vesicles in the absence of Emp46 (Figure S2). We next focused our analyses on the functional relationships between Emp47 and Ssp120.

Ssp120 requires Emp47 for proper localization

Emp47 is homologous to the mammalian cargo receptor ERGIC53, which is required for the ER export of a subset of glycoproteins including the secreted blood coagulation factors V (FV) and VIII (FVIII) (11, 12, 44, 45). ERGIC53 requires a soluble co-factor with two calcium-binding EF-hand domains, MCFD2, for the efficient transport of FV/FVIII from the ER to the ERGIC (46). The ERGIC53-MCFD2 complex is localized to the ERGIC at steady-state in a calcium-dependent manner, and ERGIC53 is required for the proper localization of MCFD2 (46, 47). While MCFD2 and Ssp120 share little sequence similarity, they share a nearly identical domain organization and lack a C-terminal KDEL/HDEL retrieval signal. The parallels between Emp47-Ssp120 and ERGIC53-MCFD2 have also been noted by Babu et al., (24). These observations combined with previous results suggesting Emp47 is required for secretion of a subset of glycoproteins led us to investigate if the Emp47-Ssp120 complex serves as a functional analog of the ERGIC53-MCFD2 complex (22).

Initial immunoblot analysis comparing wild-type and *emp47*Δ strains revealed that steady-state levels of Ssp120 were sharply reduced in *emp47*Δ cells (~16% of wild-type) (Figure 4A). To further explore the functional relationship between Emp47 and Ssp120, we performed *in vitro* COPII vesicle budding assays using microsomes prepared from wild-type, *ssp120*Δ, and *emp47*Δ cells to determine subunit interdependence (Figure 4B). In comparison to wild-type microsomes, the level of Ssp120 was greatly reduced in *emp47*Δ microsomes, which required an extended exposure to detect (Figure 4B, lanes labeled T). Importantly, the low level of Ssp120 remaining in *emp47*Δ microsomes was not efficiently packaged into COPII vesicles. In contrast, both overall levels and vesicle packaging efficiency of Emp47 were similar in wild-type and *ssp120*Δ cells. As expected, the ER resident Sec61 was not packaged whereas the ER vesicle protein Erv29 was efficiently packaged for all strains. These results indicate that ER-Golgi cycling and maintenance of steady-state levels of Ssp120 require Emp47, but loss of Ssp120 does not affect localization or trafficking of Emp47.

MCFD2 is secreted in ERGIC53-depleted mammalian cells, though a fraction may be degraded in the lysosome (equivalent to the yeast vacuole) (47). Thus, we sought to determine the fate of Ssp120 in *emp47*Δ cells. To assess secretion from cells, log-phase wild-type (untagged) and *SSP120-HA* cells with or without *emp47*Δ deletion were washed and back-diluted into fresh YPD. After 6 hr of growth at 30°C, cells were pelleted and the culture supernatant subjected to TCA-precipitation. Whole-cell lysates and TCA-

precipitated culture medium were analyzed by SDS-PAGE and immunoblot. In *emp47*Δ cells, the reduction of intracellular Ssp120-HA corresponded to a proportional increase of extracellular secreted Ssp120-HA as compared to the *EMP47* strain (Figure 4C). Interestingly, a low level of Ssp120-HA was detected in the extracellular fraction of *EMP47* cells, and may reflect a normal low level of secretion from wild type strains. As controls, the ER lumenal protein Kar2, which is also secreted at low levels (48), was detected at similar levels for all strains, and the cytoplasmic protein Sar1 was not detected in the extracellular fraction to exclude cell lysis.

During the course of our study, large-scale protein mapping approaches identified and partially characterized the Emp47-Ssp120 interaction (17, 24). Ssp120-GFP was observed to mislocalize to vacuoles by fluorescence microscopy in *emp47*Δ cells and Ssp120-HA was secreted from *emp47*Δ *vps10*Δ double mutant strains. To assess the level of Ssp120 degradation in vacuoles, we examined steady-state levels of Ssp120 in wild-type, *ssp120*Δ, and *emp47*Δ strains alone or in combination with a *PEP4* deletion. Pep4 is required for activation of most vacuolar proteases, therefore vacuolar degradation is deficient in *pep4*Δ cells (49). As shown in Figure 4D, the low Ssp120 levels in *emp47*Δ cells were increased by combining with the *pep4*Δ mutation but were not restored to wild-type levels, indicating that only a fraction of mislocalized Ssp120 traffics to the vacuole while most is secreted from cells. In contrast, the levels of Emp47 were unaffected by the *ssp120*Δ and *pep4*Δ mutations, singly or in combination. Because conditions that perturb Emp47 cycling between the ER and Golgi result in its mis-localization to the vacuole (21, 50), this provides additional evidence that Ssp120 does not influence Emp47 localization or ER-Golgi cycling. Based on these results we conclude that in the absence of Emp47, Ssp120 exits the ER via a bulk flow process and accesses later Golgi compartments where a major fraction is secreted and the remainder traffics to the vacuole for degradation. The strict requirement of Emp47 for Ssp120 localization, and the independence of Emp47 on Ssp120 for proper localization and ER-Golgi cycling, mirrors phenotypes observed in mammalian cells for the ERGIC53-MCFD2 complex and supports a model in which the Emp47-Ssp120 complex is functionally analogous (46, 47).

Phenotypic analysis of *ssp120*Δ and *emp47*Δ strains

To understand the functional relevance of the Emp47-Ssp120 interaction, we analyzed the phenotypes of *ssp120*Δ, *emp47*Δ, and double deletion mutant strains. The *emp47*Δ deletion strain was previously shown to have temperature and calcium sensitivities in certain genetic backgrounds (21, 22). We could reproduce these phenotypes in the W303a as well as the YPH500/499 backgrounds used previously (22), but did not observe these sensitivities in the BY4741/4742 or the FY833/834 backgrounds (Figure S3). Therefore, we used the W303a background for further phenotypic analysis.

The *ssp120*Δ, *emp47*Δ, and double deletion strains grew comparable to wild-type on YPD at 30°C, but displayed severe growth defects at 37°C (Figure 5A). Notably, combining the *ssp120*Δ and *emp47*Δ deletions did not exacerbate the growth defects of the single deletion mutations. The absence of synthetic negative effects in the *ssp120*Δ *emp47*Δ double deletion supports a model in which Ssp120 and Emp47 function as a complex. It is possible that

overexpression of either subunit could partially complement for function and suppress the temperature sensitive phenotype. To address this, we tested whether multi-copy expression of *EMP47* could rescue the *ssp120*Δ growth defect. As shown in Figure 5B, only multi-copy expression of *SSP120* suppressed the *ssp120*Δ growth defect at 37°C, while *ssp120*Δ temperature sensitive growth was not suppressed in strains transformed with empty vector or expressing multi-copy *EMP47*. This result is consistent with the observation that the *ssp120*Δ *emp47*Δ double deletion strain has no additive growth defect and indicates that both subunits of the Emp47-Ssp120 complex are required for function. We also noted that shifting the *ssp120*Δ and *emp47*Δ deletion strains to a restrictive temperature produced no detectable block in CPY maturation or alterations in ER-Golgi morphology (Figure S4). These observations indicate the Emp47-Ssp120 complex is not required for overall function of the secretory pathway but are more consistent with a role in biogenesis and delivery of specific cargo to their proper cellular location. Deficiencies in cargo delivery are likely the cause of thermosensitivity in *ssp120*Δ and *emp47*Δ cells.

We next asked if the *ssp120*Δ deletion influenced the Ca^{2+} sensitivity of an *emp47*Δ strain. To do this, wild-type, *ssp120*Δ, *emp47*Δ, and double deletion strains were grown on YPD supplemented with 0.25 M or 0.5 M $CaCl_2$ (Figure 5C). As with growth at 37°C, growth on 0.5 M $CaCl_2$ caused severe growth defects in *ssp120*Δ and *emp47*Δ deletion strains, but no observable synthetic effect in the double deletion strain as previously reported (24). These results are again consistent with the hypothesis that both subunits are required for a functional complex. The strong calcium phenotype also provided a means of assessing whether the HA-epitope tagged version of Ssp120 was fully functional. Growth of the *SSP120-HA* strain was indistinguishable from wild-type on 0.5 M $CaCl_2$, while *ssp120*Δ showed the expected growth defect (Figure S5).

Deletion of *SSP120* and *EMP47* suppresses the DTT sensitivity of an *ire1*Δ mutant

Emp47 is generally thought to function as a glycoprotein cargo receptor in the anterograde pathway based on its requirement for the ER-Golgi transport of Emp46, though attempts to identify Emp47-dependent secretory cargo have been unsuccessful (17, 22, 43). In searching the BioGRID database, we found multiple interactions that suggested this complex may influence glycoprotein quality control (51). Emp47 co-purified in complex with the ER quality control lectin Yos9 along with other members of the core ER-associated degradation (ERAD) machinery (52). Emp47 and Ssp120 are not glycosylated and thus not likely to be Yos9 substrates (21, 36). Deletion of *EMP47* was shown to alleviate the increased activation of the unfolded protein response (UPR) in cells with a hypomorphic allele of *KAR2* (BiP) (53). The UPR is a program of transcriptional up-regulation of ~400 genes induced by conditions that cause severe ER stress (54). In addition, a genome-wide synthetic genetic array (SGA) identified positive interactions between *SSP120* and the glycoprotein-specific Kar2 co-chaperone *SCJ1* and the UPR transducer *IRE1* (55, 56). These interactions are not due to the influence of *SSP120* and *EMP47* on the UPR because neither gene is a UPR target, nor do their deletion mutations induce the UPR, in contrast to most other known ER-Golgi anterograde cargo transporters (29, 31, 54, 57). The collective results indicate that loss of *SSP120* and *EMP47* can alleviate ER stress in a UPR-independent manner.

To further explore the connection between the Emp47-Ssp120 complex and ER stress, we examined the effects of *ssp120*Δ and *emp47*Δ mutations on cell growth under UPR-inducing conditions in wild-type and *ire1*Δ backgrounds. Because Ire1 is the sole transducer of the UPR in yeast cells, conditions of severe ER stress that activate the UPR are lethal to *ire1*Δ cells, thus potential masking effects are removed in this background (58). Growth of wild-type (BY4742) or *ire1*Δ cells in combination with *ssp120*Δ or *emp47*Δ mutations was assessed on YPD supplemented with either the reducing agent DTT or the *N*-glycosylation inhibitor tunicamycin, both known to induce the UPR (Figure 6A). Under both conditions, growth of the *ssp120*Δ and *emp47*Δ strains was comparable to wild-type cells, while the *ire1*Δ strain showed the expected growth defects. Interestingly, *ssp120*Δ or *emp47*Δ rescued the growth defect of *ire1*Δ cells on DTT, but not on tunicamycin. In contrast, we did not detect suppression of *ire1*Δ sensitivity to DTT when combined with *emp46*Δ (not shown). These results suggest that *ssp120*Δ and *emp47*Δ mutations alleviate ER stress in the presence of widespread protein misfolding induced by reducing agents in an *N*-glycosylation dependent manner.

Why might the loss of the Emp47-Ssp120 complex benefit cells during severe ER stress? Under normal growth conditions, misfolded glycoproteins are proposed to traffic from the ER to the Golgi at a low rate, followed by retrieval to the ER for additional rounds of folding or for degradation (59–64). The mammalian Emp47 homolog and ERGIC53 family member VIP36 is proposed to function in this retrieval pathway, which in combination with the observations above raised the possibility that in yeast the Emp47-Ssp120 complex may also act in a post-ER quality control retrieval pathway (65–67). In this scenario, loss of Emp47-Ssp120 function could alleviate DTT-induced toxicity in an *ire1*Δ background by permitting clearance of misfolded glycoproteins from the ER for delivery and degradation in the vacuole (63, 68, 69).

To address this question, we first examined if the turnover rate of a model ERAD substrate such as CPY* (70) was altered in the *ssp120*Δ and *emp47*Δ strains. We reasoned that if the Emp47-Ssp120 complex acted in retrieval of misfolded glycoproteins, then turnover rates would be delayed because escaped CPY* would slowly transit later branches of the secretory pathway before degradation in the vacuole (68). However, under the conditions of our analysis we did not detect changes in CPY* turnover rates in the *ssp120*Δ or *emp47*Δ strains (Figure S6). To rule out cargo specific effects, we examined turnover rates of other model ERAD substrates and did not observe delays in Gas1* (Figure S7) or PrA* (not shown) degradation rates in *ssp120*Δ or *emp47*Δ backgrounds. We also considered the possibility that the fraction of ERAD substrate that escaped the ER quality control machinery and depended on post-ER retrieval would be quite small and undetectable by this method. Therefore we used an alternative approach to saturate the ERAD pathway through *GAL1*-regulated overexpression of CPY*, which has been shown to induce the UPR and produce ER toxicity in *ire1*Δ cells (68, 70, 71). If the Emp47-Ssp120 complex retrieves misfolded glycoproteins from Golgi compartments we expected their deletion to partially suppress toxicity of overexpressed CPY* in an *ire1*Δ sensitized background. However, we observed that CPY* overexpression in the *ssp120*Δ *ire1*Δ and *emp47*Δ *ire1*Δ double deletion strains grew as poorly as the *ire1*Δ strain, while growth of the *ssp120*Δ and *emp47*Δ strains

was comparable to wild-type (Figure 6B). These findings indicate that the Emp47-Ssp120 complex does not function in retrieval of misfolded glycoproteins from Golgi compartments as proposed for other ERGIC53 family members.

Synthetic Genetic Array Analysis of *emp47*Δ

To gain further insight into Emp47 cellular function, we performed an SGA analysis (72) in which the *emp47*Δ mutation was combined individually with all other non-essential gene deletions (~4,900 yeast strains) and screened for growth phenotypes. After comparing growth of the double deletion strains on YPD medium at 30°C, we identified 29 gene deletions that produced synthetic negative growth phenotypes when combined with *emp47*Δ in three independent rounds of screening (Table S2). These gene interactions were ranked based on colony size with more negative scores indicating stronger synthetic negative interactions (73).

Top hits from this screen were independently tested by constructing double deletion mutants in the BY4742 strain background. We observed that the *emp47*Δ *gas1*Δ and *emp47*Δ *mnn11*Δ strains displayed synthetic negative growth phenotypes compared to the individual deletion mutants (Figure 7), whereas combinations with *yta12*Δ and *ste50*Δ did not produce detectable growth phenotypes under our standard conditions. Interestingly both Gas1 and Mnn11 influence cell wall assembly in yeast. Gas1 is an abundant 1,3-β-glucanosyltransferase that is GPI anchored at the cell surface and catalyzes formation of the yeast cell wall (74, 75). Mnn11 is a subunit of the major Golgi-localized α1,6-mannosyltransferase complex that elongates core-type N-glycans necessary for biogenesis of cell wall components (76, 77). Importantly, pairwise combination of *ssp120*Δ with *gas1*Δ or *mnn11*Δ also resulted in synthetic negative growth phenotypes that were indistinguishable from the *emp47*Δ double mutants and provide further evidence that Emp47 and Ssp120 operate as a functional unit. These collective findings support a model in which the Emp47-Ssp120 complex acts in efficient anterograde transport of cell surface glycoproteins necessary for cell wall integrity.

Discussion

A comprehensive proteomic analysis of purified COPII vesicles provided an inventory of transport machinery and secretory cargo packaged into these trafficking intermediates. Several of the identified polypeptides corresponded to previously characterized vesicle proteins that link secretory cargo to coat subunits during the ER budding stage or proteins that operate in vesicle targeting and membrane fusion (10, 19, 31). Three newly identified polypeptides exhibited the properties of other ER vesicle proteins but are of poorly defined function. We confirmed that Coy1, Sly41 and Ssp120 are efficiently packaged into COPII vesicles and given their subcellular distribution we propose these proteins function in transport through the early secretory pathway. We further characterized the Ssp120 protein in this report.

Purification of Ssp120 revealed an apparent stoichiometric complex with Emp47, a membrane protein known to cycle between the ER and Golgi and thought to transport glycoproteins in a manner similar to its mammalian homolog ERGIC53. Emp46 was

detected as a minor component of this complex. In *emp47*Δ cells, most Ssp120 was secreted into the extracellular media indicating a requirement for Emp47 in Ssp120 localization. We observed that deletion of *emp47*Δ or *ssp120*Δ produced identical calcium and temperature sensitive phenotypes further supporting function as complex. No detectable trafficking or growth phenotypes were associated with the *emp46*Δ cells. SGA analysis revealed synthetic negative interactions between *emp47*Δ and genes that encode abundant cell wall proteins or machinery needed for proper glycosylation of cell wall components. The *ssp120*Δ deletion displayed the same pattern of synthetic genetic interactions. Based on these findings we conclude that both Emp47 and Ssp120 are required for this complex to function, and that the Emp47-Ssp120 complex acts as a shuttling cargo receptor in the early secretory pathway for efficient biogenesis and transport of cell surface glycoproteins. Emp46 may play a role as a cargo specific adaptor of the Emp47-Ssp120 complex.

During the course of our studies, two high-throughput reports also identified and partially characterized interactions between Emp47 and Ssp120. Herzig and colleagues reported mislocalization of Ssp120-GFP in microscopy screens to pair potential cargo receptors, including Emp47, with specific cargo proteins (17). In addition, Babu et al. identified Ssp120 associated with Emp47 and Emp46 in a global analysis of yeast membrane proteins by affinity purification and mass spectrometry analysis (24). Moreover, the investigators confirmed these interactions through tagging and immunoprecipitation approaches and demonstrated calcium sensitivity of the *ssp120*Δ strain. Interestingly, Ssp120-GFP was observed to accumulate in the vacuole of *emp47*Δ cells and Ssp120-HA was secreted from cells when the vacuole sorting receptor Vps10 was deleted in an *emp47*Δ background (24). Using different assays we found that most Ssp120 was secreted from *emp47*Δ cells and that a smaller fraction reaches the vacuole where it can be stabilized in a *pep4*Δ background. Our current work is largely consistent with and extends these published findings.

Our observation that combining the *emp47*Δ or *ssp120*Δ deletion with *ire1*Δ suppressed sensitivity to DTT is intriguing. In contrast, other anterograde cargo receptors display synthetic negative interactions with *ire1*Δ as buildup of cargo in the ER is thought to be managed by an activated UPR (29, 55, 57). In addition, our results indicate that Emp47-Ssp120 does not function in the clearance of misfolded proteins such as CPY* from the early secretory pathway to alleviate ER stress. However, we note that genome wide analyses turned up both *emp47*Δ and *ssp120*Δ as constitutive activators of the yeast cell wall integrity pathway (78). Here, phosphorylation of the yeast mitogen-activated protein kinase (MAPK) Slt2 was increased 4 to 5-fold in *emp47*Δ and *ssp120*Δ cells. Activated Slt2 turns on a transcriptional program that increases expression of cell wall proteins and biogenesis machinery (79). Additional studies have shown that activated Slt2 helps manage ER stress in processes that are both Ire1-dependent (80) and independent (81, 82). Cell wall integrity issues in *emp47*Δ and *ssp120*Δ strains are also consistent with our SGA screen, which identified synthetic negative interactions with genes involved in cell wall assembly. Based on these collective findings, we propose that cells lacking Emp47-Ssp120 complex have only a low level of nascent secretory proteins accumulating in the ER but that inefficient delivery of cell surface glycoproteins diminishes cell wall integrity. To compensate, these cells constitutively activate Slt2 signaling networks, which partially overlap with targets of

the unfolded protein response pathway to alleviate sensitivity to DTT in the absence of Ire1 function. However, we could not detect clear phenotypic consequences from combining *slt2*Δ with *emp47*Δ and further studies are needed to support this model.

How does Emp47-Ssp120 complex function compare to the mammalian ERGIC53-MCDF2 complex? Emp47 shares low sequence identity (18.4%) but overall high structural conservation with ERGIC53 (23, 83). These proteins belong to the L-type lectin family, which fold into β-sandwich structures and contain defined carbohydrate recognition domains (83, 84). However, there are distinct differences between Emp47 and ERGIC53 in that Emp47 does not appear to bind Ca^{2+} directly and a conserved histidine residue involved in pH-regulated binding of *N*-linked glycans to ERGIC53 is absent in Emp47 (23, 83, 85). Moreover, the putative Ca^{2+} binding protein Ssp120 and the known calcium binding protein MCFD2 associated with Emp47 and ERGIC53, respectively, are also distinct. While both proteins contain hydrophobic signal sequences and dual EF-hand motifs, the 234 amino acid Ssp120 protein and 146 amino acid MCFD2 protein share low sequence identity overall. In fact, Ssp120 shares higher sequence identity (31% over 95 residues) with nucleobindin-1, another Golgi-localized calcium-binding protein (39). Therefore it is possible that the Emp47-Ssp120 complex is more analogous to other ERGIC53 family members such as Vip36 and VIPL (86), which could function in complex with associated nucleobindin proteins. A recent chemical proteomic analysis also revealed a role for nucleobindin-1 in lipid metabolism, possibly functioning as a carrier of specific fatty acid amides (87). Thus an alternative model might be that these complexes traffic lipids, which could also explain altered cell wall properties in yeast *emp47*Δ and *ssp120*Δ mutants.

In humans, the calcium-binding MCFD2 subunit is thought to act as a cargo specificity factor to bind the blood clotting factors V and VIII to ERGIC53 for their efficient export from the ER (88). Whereas other secretory cargo, including cathespin Z and cathepsin C, appear not to depend on the MCFD2 subunit (47). Biochemical and structural studies have shown that high-mannose oligosaccharides bind directly to the ERGIC53 carbohydrate recognition domain (CRD) in the absence of MCFD2 (86, 89, 90) leading to a model where the CRD of ERGIC53 binds *N*-linked glycans attached to nascent secretory proteins and the MCFD2 subunit interacts with nearby peptide residues within specific cargo proteins (89). However, structural studies have not confirmed the molecular basis of this dual interaction. Both pH and Ca^{2+} concentrations influence cargo interactions with ERGIC53-MCFD2 and are thought to promote cargo binding in the ER and release in intermediate or early Golgi compartments (85, 91, 92). In yeast, phenotypes of the *emp47*Δ and *ssp120*Δ deletion strains are indistinguishable; therefore, we propose that this complex acts as a functional unit for ER export of specific cell surface glycoproteins. Compartmental pH and/or Ca^{2+} levels are also likely to regulate cargo binding to Emp47-Ssp120 in yeast. Studies guided by this simplified model should allow for a full mechanistic dissection of how this family of L-type lectins with their putative calcium-binding subunits can recognize glycoproteins in the ER and then release bound cargo in post-ER compartments.

Materials and Methods

Yeast strains and media

Yeast strains used in this study are listed in Table S3. Standard yeast methods were used (93). DNA for plasmid constructions and yeast transformation was generated using the Phusion High-Fidelity PCR system (Thermo Scientific, Rockford, IL). Oligonucleotide primers (IDT DNA, Coralville, IA) are listed in Supplemental Table S4. Yeast cells were transformed by the high-efficiency lithium acetate technique (94).

BY4742-background deletion mutants containing the *kanMX4* cassette were purchased from Research Genetics (Invitrogen, Carlsbad, CA). *C*-terminal 3xHA-epitope tagged strains and deletion mutants containing the *HIS3MX6* cassette were created using described methods (40). To generate CBY3296 and CBY3328, the *emp47*Δ*::kanMX4* cassette and flanking regions were PCR amplified from CBY1299 with primers NMp30 and NMp31 and transformed into W303a and SEY6210, respectively. Strains in which the *SEC7* and *SEC21* genes were replaced with *SEC7-GFPx3* and *SEC21-GFPx3*, respectively, were constructed as previously described (95). The above mutations were confirmed by immunoblot and colony PCR (check primer sequences available upon request). The *pep4*Δ*::URA3* mutation in CBY3564, CBY3565, and CBY3566 was achieved using linearized plasmid pTS15 as previously described (96). Deletion of *PEP4* in these strains was confirmed by immunoblot for CPY processing.

Unless otherwise noted, cells were grown at 30°C in rich medium (YPD: 1% yeast extract, 1% peptone, and 2% dextrose) or in synthetic complete medium (SC: 0.67% yeast nitrogen base without amino acids, 2% dextrose, and appropriate amino acid supplement mixture [CSM; MP Biomedicals, Solon, OH]). SR and SG media are SC except with 3% raffinose or 2% galactose, respectively, instead of 2% dextrose. For growth of W303a–background strains, media was supplemented with 40 μg/mL adenine. For overexpression of CPY*HA from the *GAL1/10* promoter (pES28) for the growth assay shown in Figure 6B, strains were grown at 30°C to saturation in SR-Ura and adjusted to an OD_{600} of 1.0. A 10-fold dilution series was spotted onto SC-Ura, SG-Ura, or SC-Ura with 2% galactose and 0.2% dextrose and incubated at 30°C for 3 days.

Plasmids

Plasmids used in this study are listed in Supplemental Table S5. The sequences for *EMP47* (YFL048c) and *SSP120* (YLR250w) were from the Saccharomyces Genome Database (http:/www.yeastgenome.org/). The *EMP47* coding sequence and ~440 bp each upstream and downstream regions were amplified from BY4742 genomic DNA with primers NMp28 and NMp29. *Eco*RI and *Hind*III sites appended by the primers were used to clone this fragment into the same sites on pRS316 (*CEN*, *URA3*) (97) to generate pNM4 as an intermediate step. Plasmid pNM4 was digested with *Spe*I and *Hind*III (both cleave in the polylinker of pRS316) and the fragment containing *EMP47* subcloned into pRS425 (2μ, *LEU2*) (98), creating plasmid pNM23. The *SSP120* coding sequence and ~450 bp flanking regions were amplified from BY4742 genomic DNA and primers NMp24 and NMp66. *Not*I and *Bam*HI sites introduced by the primers were used to insert this fragment into the same

sites on pRS313 (*CEN*, *HIS3*) (97) to create plasmid pNM13 as an intermediate step. Plasmid pNM13 was digested with *Not*I and *Sal*I (both cleave in the pRS313 polylinker) and the fragment containing *SSP120* was subcloned into the same sites on pRS425 (2μ, *LEU2*) (98).

To construct the 6xHis-tagged N-terminal fusion protein with mature Ssp120 (Ssp120Δss) for bacterial expression, the *SSP120* coding sequence after the signal peptide (a.a. 23–234) was amplified from plasmid pNM13 with primers NMp81 and NMp82. These primers introduced a silent T to C mutation in nucleotide 84 to destroy an endogenous *Ase*I site, and appended 5' *Ase*I and 3' *Bam*HI sites for insertion into the *Nde*I and *Bam*HI sites of pET-15b (Novagen, Billerica, MA) to create plasmid pNM18 (*Ase*I and *Not*I have compatible ends that ligate in-frame). All generated constructs were verified by restriction digest and sequencing. Plasmids pDN436 (71), pES28 (68), and pJK59 (99) were previously described. Briefly, pDN436 encodes HA epitope-tagged CPY* under control of the *PRC1* promoter in pRS315, pES28 encodes CPY*HA under control of the *GAL1/10* promoter in YCp50, and pJK59 (*CEN*, *URA3*) encodes Sec63-GFP under control of the *SEC63* promoter.

Antibodies

Polyclonal antibodies were raised against recombinant 6His-Ssp120Δss expressed from pNM18 in *E. coli* C43(DE3) cells (Lucigen, Middleton, WI). After a 3 h induction with 1 mM isopropyl β-D-thiogalactoside, the fusion protein was purified from the soluble extract on a Ni-NTA column (Qiagen, Valencia, CA) as recommended by the manufacturer. Purified protein was used to immunize rabbits by standard procedures (Covance, Denver, PA). For immunoblotting, anti-Ssp120 antiserum was diluted to 1:2000. Polyclonal antibodies against Sec61 (100), Erv29 (15), carboxypeptidase Y (CPY) (101), Emp47 (21), Gas1 (102), Och1 (19), Yet3 (103), Cdc48 (104), Sar1 (105), and Kar2 (106) were described earlier. Monoclonal anti-HA (HA.11) antibody was obtained from Covance (Princeton, NJ).

Yeast cell lysates and immunoblotting

To assess steady-state protein levels, 2 OD_{600} equivalent of mid-log cells was harvested by low-speed centrifugation and the pellets flash-frozen in liquid nitrogen. Cell pellets were thawed on ice and resuspended in 200 μL of 20 mM NaN_3 with 1 mM phenylmethylsulfonyl fluoride. Glass beads (BioSpec, Bartlesville, OK) and 200 μL 5× SDS-PAGE sample buffer were added before lysis at 4°C using a Mini-Beadbeater-16 (BioSpec). Samples were heated for 5 min at 95°C, cleared by centrifugation for 3 min at 14,000 × *g*, and resolved by SDS-PAGE. Immunoblots were developed with Supersignal Pico chemiluminescent substrate (Pierce Chemical, Rockford, IL), imaged using a G:BOX Chemi XR5 (Syngene, Frederick, MD), and quantified with GeneTools image analysis software (Syngene). Statistical analyses were performed with Prism (Graphpad, La Jolla, CA) or Excel (Microsoft, Redmond, Wa).

In vitro vesicle budding and transport assays

Preparative scale synthesis of COPII vesicles was performed by incubating microsomes derived from wild-type (BY4742) cells with ATP and GTP in the presence (+COPII) or absence (−COPII) of purified Sar1, Sec23-Sec24 complex and Sec13-Sec31 complex as described previously (19, 25, 26). Budding reactions (300 μL volume) were subjected to

centrifugation at 4°C for 3 min at 14,000 × *g* to separate vesicles from heavier donor membranes. Vesicles contained in this medium-speed supernatant retain a substantial amount of COPII proteins that could interfere with the identification of less-abundant ER vesicle proteins by mass spectrometry. To strip COPII proteins from the vesicles by flotation through a Nycodenz gradient, 270 μL of this medium-speed supernatant was mixed with 400 μL of 60% Nycodenz (in D_2O) and transferred to the bottom of a TLS-55 centrifuge tube (Beckman Coulter, Danvers, MA). Next, 450 μL each of 25% and 20% Nycodenz (in D_2O with 20 mM HEPES pH 7.5, 150 mM potassium acetate, and 5 mM magnesium acetate) were layered on top, followed by 750 μL of buffer B88 (20 mM HEPES pH 7.0, 250 mM sorbitol, 150 mM potassium acetate, and 5 mM magnesium acetate). The gradients were centrifuged at 4°C for 3 h at 166,000 × *g* in a TLS-55 rotor. To detect the peak vesicle-containing fractions, budding reactions were initially performed in the presence of in vitro-produced ^{35}S-labeled pro-α-factor. The top 250 μL of each gradient was discarded, and 100 μL fractions collected and radioactivity measured to determine the α-factor peak. A COPII-dependent peak of radioactivity was reproducibly observed in fraction 7, with activity in fractions 5 to 8.

For *en bloc* mass spectrometry, the addition of ^{35}S-labeled pro-α-factor was omitted and the peak α-factor fractions (5 to 8) determined above were collected. These fractions were pooled, mixed with 800 μL of B88, and the vesicles were pelleted by centrifugation at 4°C for 15 min at 152,000 × *g* in a TLA-100.3 rotor (Beckman Coulter). Pellets were solubilized in 40 μL of 5× sample buffer by heating for 4 min at 75°C, and then resolved 17 mm (measured from bottom of well to dye front) into a pre-cast 12% Novex Tris-glycine gel (Invitrogen). Proteins were stained with a Colloidal Blue Staining Kit according to the manufacturer's instructions (Invitrogen), and the sample lanes were cut into three sections corresponding to 95–250 kDa, 55–95 kDa, and 55 kDa to the dye front as shown in Figure 1B. These gel sections were submitted to the Taplin Mass Spectrometry Facility (Harvard Medical School, Boston, MA) for peptide sequence analysis by microcapillary LC/MS/MS.

Analytical scale budding reactions to assess COPII-dependent packaging efficiency by immunoblot from semi-intact cells and microsomes incubated in the presence or absence of purified COPII components were performed as described (19, 25). The in vitro assay to measure overall ER-to-Golgi transport efficiency following ^{35}S-glyco-pro-α-factor (Supplementary Figure S1) was performed as previously described (41). The data plotted in this experiment are the average of duplicate determinations and the error bars represent the range.

Immunoprecipitation experiments

For native immunoprecipitations, 200 μL of microsomes (0.25 mg of total membrane protein) were solubilized on ice with 1 mL of IP buffer (15 mM Tris-HCl, pH 7.5, 150 mM NaCl, 1% Triton X-100, 1 mM phenylmethylsulfonyl fluoride) for 10 min. Triton-insoluble material was removed by centrifugation at 4°C for 5 min at 14,000 × *g*, and 1 mL of cleared supernatant (total input) was combined with 30 μL of 20% protein A-Sepharose (GE Healthcare, Piscataway, NJ) and 1 μg of anti-HA.11 antibody (Covance) or 1 uL anti-Ssp120 antiserum for each immunoprecipitation. The reactions were incubated for 2 h at

4°C with rotation, and the unbound protein fraction (1 mL) was discarded. The precipitates were washed five times with cold IP buffer and were eluted from the beads by adding 30 μL of 5× sample buffer and heating for 5 min at 75°C. Samples were resolved by SDS-PAGE and proteins visualized by immunoblot or silver stain. For identification of the Ssp120-HA–binding protein, native immunoprecipitations were performed as above except using 0.40 mg of microsomes. Samples were resolved on a pre-cast 10% Novex Tris-glycine gel (Invitrogen) and proteins visualized using a Colloidal Blue Staining Kit according to the manufacturer's instructions (Invitrogen). The band of interest was excised and submitted for peptide analysis at the Taplin Mass Spectrometry Facility (Harvard Medical School) as described above.

Ssp120-HA secretion assay

The protocol to analyze extracellular Ssp120-HA secretion into the culture media was adapted from a Kar2 secretion assay (29). Saturated cultures were back-diluted into YPD and grown to mid-logarithmic phase. Cells were then harvested, washed twice in sterile water, and resuspended in fresh YPD at equivalent cell densities (OD_{600}=0.1). After 6 h growth, 1.5 mL of the cultures was centrifuged for 5 min at 14,000 × *g* and 1.35 mL of the supernatant was transferred to a new tube. Extracellular proteins were precipitated from the supernatant by adding cold 100% trichloroacetic acid to a final concentration of 10% and incubating on ice for 20 min. The precipitate was collected by centrifugation at 4°C for 15 min at 14,000 × *g*, washed with 1 mL of cold 100% acetone, and air-dried at room temperature. Precipitated proteins were resuspended in 40 μL of 5× sample buffer supplemented with 50 mM Tris, pH 9.4, heated for 5 min at 75°C, and 10 μL resolved by SDS-PAGE and visualized by immunoblot. The cell pellets from the 1.5 mL culture were resuspended in 200 μL of lysis buffer (0.1 M sorbitol, 20 mM HEPES, pH 7.4, 50 mM KOAc, 2 mM EDTA, 1 mM dithiothreitol, 1 mM phenylmethylsulfonyl fluoride) and were lysed with glass beads by vortexing at 4°C for 10 min. Lysates were cleared by centrifugation at 4°C for 3 min at 3,500 × *g* and 200 μL of the supernatant transferred to a new tube. This supernatant was mixed with 200 μL of 5× sample buffer, heated for 5 min at 75°C, and 10 μL resolved by SDS-PAGE and visualized by immunoblot.

Live-cell microscopy

Strains expressing recombinant GFP-fusion proteins were grown at 30°C in SC-Ura to mid-log. Cultures were then back-diluted into fresh, pre-warmed SC-Ura in duplicate and incubated for 6 h at 30°C (permissive) or 37°C (restrictive). Cells were imaged at room temperature in liquid medium under a coverslip using a Deltavision Imaging System (Applied Precision, Issaquah, WA) composed of a customized Olympus (Center Valley, PA) IX-71 inverted wide-field microscope, a UPlanS Apochromatic 100×/1.40 NA lens, a Photometrics (Tucson, AZ) CoolSNAP HQ2 camera, and an InsightSSI (Applied Precision) solid-state illumination unit. Images were captured as Z-series with 0.2 μm step-size, and processed by iterative deconvolution in SoftWoRx (Applied Precision) and then analyzed and maximum-intensity projections of the z-stacks generated in ImageJ (National Institutes of Health, Bethesda, MD). For the differential interference contrast (DIC) images, a single focal plane in the center of the cells was used.

Cycloheximide decay assays

Cycloheximide decay assays were performed according to (107) with modifications. Strains expressing CPY*HA from pDN436 were grown to saturation in SC-Leu. Cultures were back-diluted into YPD and grown to OD_{600} = 0.8–1.2, then harvested and concentrated to 2 OD_{600} per mL in fresh, pre-warmed YPD. Protein translation was stopped by addition of CHX to a final concentration of 1 mg/mL. At the indicated time points, 1 mL culture was aliquoted into 300 μL of 50 mM NaN_3 on ice, centrifuged at 4°C for 1 min at 14,000 × *g*, and the pellets flash frozen in liquid N_2. Pellets were processed as described above for whole-cell lysates.

Synthetic genetic array (SGA) analysis

SGA screening was conducted as described (72) with some modifications (73) using a Singer ROTOT HDA (Singer Instruments). The *emp47*Δ query strain CBY3663 (*emp47*Δ::*NatMX4*, constructed in Y7092) was mated to the yeast haploid deletion collection (each gene deleted with KanMX cassette confers resistance to G418), diploids selected and sporulated, followed by selection of double mutant haploids. The automated software HT Colony Grid Analyzer (108) was used to measure colony sizes after growth at 30°C, and raw values were calculated relative to the median colony size of the plate. Three independent rounds of screening were conducted and for synthetic negative interactions that reproduced in all three rounds, the data were averaged and ranked by strength of the effect (the larger the negative number, the stronger the interaction). We used GO Term Finder to identify significant gene ontology (GO) terms enriched as hits in the screen (109).

Supplementary Material

Refer to Web version on PubMed Central for supplementary material.

Acknowledgments

We thank Davis Ng for the GAL1-CPY* plasmid and Yoshifumi Jigami for the HA-Gas1* plasmid. This work was supported by the National Institutes of Health grants R37GM052549 (C.B.), R01NS065317 (A.G.) and K12-GM088033 (N.D.).

References

1. Barlowe CK, Miller EA. Secretory protein biogenesis and traffic in the early secretory pathway. Genetics. 2013; 193(2):383–410. [PubMed: 23396477]
2. Kuehn MJ, Herrmann JM, Schekman R. COPII-cargo interactions direct protein sorting into ER-derived transport vesicles. Nature. 1998; 391(6663):187–190. [PubMed: 9428766]
3. Miller EA, Beilharz TH, Malkus PN, Lee MC, Hamamoto S, Orci L, Schekman R. Multiple cargo binding sites on the COPII subunit Sec24p ensure capture of diverse membrane proteins into transport vesicles. Cell. 2003; 114(4):497–509. [PubMed: 12941277]
4. Orci L, Ravazzola M, Meda P, Holcomb C, Moore HP, Hicke L, Schekman R. Mammalian Sec23p homologue is restricted to the endoplasmic reticulum transitional cytoplasm. Proceedings of the National Academy of Sciences of the United States of America. 1991; 88(19):8611–8615. [PubMed: 1924322]
5. Rossanese OW, Soderholm J, Bevis BJ, Sears IB, O'Connor J, Williamson EK, Glick BS. Golgi structure correlates with transitional endoplasmic reticulum organization in Pichia pastoris and Saccharomyces cerevisiae. The Journal of cell biology. 1999; 145(1):69–81. [PubMed: 10189369]

6. Bannykh SI, Rowe T, Balch WE. The organization of endoplasmic reticulum export complexes. The Journal of cell biology. 1996; 135(1):19–35. [PubMed: 8858160]
7. Matsuoka K, Orci L, Amherdt M, Bednarek SY, Hamamoto S, Schekman R, Yeung T. COPII-coated vesicle formation reconstituted with purified coat proteins and chemically defined liposomes. Cell. 1998; 93(2):263–275. [PubMed: 9568718]
8. Stagg SM, Gurkan C, Fowler DM, LaPointe P, Foss TR, Potter CS, Carragher B, Balch WE. Structure of the Sec13/31 COPII coat cage. Nature. 2006; 439(7073):234–238. [PubMed: 16407955]
9. Lee MC, Miller EA, Goldberg J, Orci L, Schekman R. Bi-directional protein transport between the ER and Golgi. Annual review of cell and developmental biology. 2004; 20:87–123.
10. Dancourt J, Barlowe C. Protein sorting receptors in the early secretory pathway. Annual review of biochemistry. 2010; 79:777–802.
11. Nichols WC, Seligsohn U, Zivelin A, Terry VH, Hertel CE, Wheatley MA, Moussalli MJ, Hauri HP, Ciavarella N, Kaufman RJ, Ginsburg D. Mutations in the ER-Golgi intermediate compartment protein ERGIC-53 cause combined deficiency of coagulation factors V and VIII. Cell. 1998; 93(1):61–70. [PubMed: 9546392]
12. Appenzeller C, Andersson H, Kappeler F, Hauri HP. The lectin ERGIC-53 is a cargo transport receptor for glycoproteins. Nature cell biology. 1999; 1(6):330–334. [PubMed: 10559958]
13. Appenzeller-Herzog C, Nyfeler B, Burkhard P, Santamaria I, Lopez-Otin C, Hauri HP. Carbohydrate- and conformation-dependent cargo capture for ER-exit. Molecular biology of the cell. 2005; 16(3):1258–1267. [PubMed: 15635097]
14. Muniz M, Nuoffer C, Hauri HP, Riezman H. The Emp24 complex recruits a specific cargo molecule into endoplasmic reticulum-derived vesicles. The Journal of cell biology. 2000; 148(5): 925–930. [PubMed: 10704443]
15. Belden WJ, Barlowe C. Role of Erv29p in collecting soluble secretory proteins into ER-derived transport vesicles. Science (New York, NY). 2001; 294(5546):1528–1531.
16. Powers J, Barlowe C. Transport of axl2p depends on erv14p, an ER-vesicle protein related to the Drosophila cornichon gene product. The Journal of cell biology. 1998; 142(5):1209–1222. [PubMed: 9732282]
17. Herzig Y, Sharpe HJ, Elbaz Y, Munro S, Schuldiner M. A systematic approach to pair secretory cargo receptors with their cargo suggests a mechanism for cargo selection by Erv14. PLoS biology. 2012; 10(5):e1001329. [PubMed: 22629230]
18. Stamnes MA, Craighead MW, Hoe MH, Lampen N, Geromanos S, Tempst P, Rothman JE. An integral membrane component of coatomer-coated transport vesicles defines a family of proteins involved in budding. Proceedings of the National Academy of Sciences of the United States of America. 1995; 92(17):8011–8015. [PubMed: 7644530]
19. Otte S, Belden WJ, Heidtman M, Liu J, Jensen ON, Barlowe C. Erv41p and Erv46p: new components of COPII vesicles involved in transport between the ER and Golgi complex. The Journal of cell biology. 2001; 152(3):503–518. [PubMed: 11157978]
20. Breuza L, Halbeisen R, Jeno P, Otte S, Barlowe C, Hong W, Hauri HP. Proteomics of endoplasmic reticulum-Golgi intermediate compartment (ERGIC) membranes from brefeldin A-treated HepG2 cells identifies ERGIC-32, a new cycling protein that interacts with human Erv46. The Journal of biological chemistry. 2004; 279(45):47242–47253. [PubMed: 15308636]
21. Schroder S, Schimmoller F, Singer-Kruger B, Riezman H. The Golgi-localization of yeast Emp47p depends on its di-lysine motif but is not affected by the ret1-1 mutation in alpha-COP. The Journal of cell biology. 1995; 131(4):895–912. [PubMed: 7490292]
22. Sato K, Nakano A. Emp47p and its close homolog Emp46p have a tyrosine-containing endoplasmic reticulum exit signal and function in glycoprotein secretion in Saccharomyces cerevisiae. Molecular biology of the cell. 2002; 13(7):2518–2532. [PubMed: 12134087]
23. Satoh T, Sato K, Kanoh A, Yamashita K, Yamada Y, Igarashi N, Kato R, Nakano A, Wakatsuki S. Structures of the carbohydrate recognition domain of Ca2+-independent cargo receptors Emp46p and Emp47p. The Journal of biological chemistry. 2006; 281(15):10410–10419. [PubMed: 16439369]

24. Babu M, Vlasblom J, Pu S, Guo X, Graham C, Bean BD, Burston HE, Vizeacoumar FJ, Snider J, Phanse S, Fong V, Tam YY, Davey M, Hnatshak O, Bajaj N, et al. Interaction landscape of membrane-protein complexes in Saccharomyces cerevisiae. Nature. 2012; 489(7417):585–589. [PubMed: 22940862]
25. Barlowe C, Orci L, Yeung T, Hosobuchi M, Hamamoto S, Salama N, Rexach MF, Ravazzola M, Amherdt M, Schekman R. COPII: a membrane coat formed by Sec proteins that drive vesicle budding from the endoplasmic reticulum. Cell. 1994; 77(6):895–907. [PubMed: 8004676]
26. Belden WJ, Barlowe C. Erv25p, a component of COPII-coated vesicles, forms a complex with Emp24p that is required for efficient endoplasmic reticulum to Golgi transport. The Journal of biological chemistry. 1996; 271(43):26939–26946. [PubMed: 8900179]
27. Cao X, Barlowe C. Asymmetric requirements for a Rab GTPase and SNARE proteins in fusion of COPII vesicles with acceptor membranes. The Journal of cell biology. 2000; 149(1):55–66. [PubMed: 10747087]
28. Todorow Z, Spang A, Carmack E, Yates J, Schekman R. Active recycling of yeast Golgi mannosyltransferase complexes through the endoplasmic reticulum. Proceedings of the National Academy of Sciences of the United States of America. 2000; 97(25):13643–13648. [PubMed: 11095735]
29. Belden WJ, Barlowe C. Deletion of yeast p24 genes activates the unfolded protein response. Molecular biology of the cell. 2001; 12(4):957–969. [PubMed: 11294899]
30. Heidtman M, Chen CZ, Collins RN, Barlowe C. A role for Yip1p in COPII vesicle biogenesis. The Journal of cell biology. 2003; 163(1):57–69. [PubMed: 14557247]
31. Bue CA, Bentivoglio CM, Barlowe C. Erv26p directs pro-alkaline phosphatase into endoplasmic reticulum-derived coat protein complex II transport vesicles. Molecular biology of the cell. 2006; 17(11):4780–4789. [PubMed: 16957051]
32. Gillingham AK, Pfeifer AC, Munro S. CASP, the alternatively spliced product of the gene encoding the CCAAT-displacement protein transcription factor, is a Golgi membrane protein related to giantin. Molecular biology of the cell. 2002; 13(11):3761–3774. [PubMed: 12429822]
33. Dascher C, Ossig R, Gallwitz D, Schmitt HD. Identification and structure of four yeast genes (SLY) that are able to suppress the functional loss of YPT1, a member of the RAS superfamily. Molecular and cellular biology. 1991; 11(2):872–885. [PubMed: 1990290]
34. Ossig R, Dascher C, Trepte HH, Schmitt HD, Gallwitz D. The yeast SLY gene products, suppressors of defects in the essential GTP-binding Ypt1 protein, may act in endoplasmic reticulum-to-Golgi transport. Molecular and cellular biology. 1991; 11(6):2980–2993. [PubMed: 1903839]
35. Huh WK, Falvo JV, Gerke LC, Carroll AS, Howson RW, Weissman JS, O'Shea EK. Global analysis of protein localization in budding yeast. Nature. 2003; 425(6959):686–691. [PubMed: 14562095]
36. Sidhu RS, Mathewes S, Bollon AP. Selection of secretory protein-encoding genes by fusion with PHO5 in Saccharomyces cerevisiae. Gene. 1991; 107(1):111–118. [PubMed: 1743509]
37. Inadome H, Noda Y, Adachi H, Yoda K. Immunoisolaton of the yeast Golgi subcompartments and characterization of a novel membrane protein, Svp26, discovered in the Sed5-containing compartments. Molecular and cellular biology. 2005; 25(17):7696–7710. [PubMed: 16107716]
38. Miura K, Titani K, Kurosawa Y, Kanai Y. Molecular cloning of nucleobindin, a novel DNA-binding protein that contains both a signal peptide and a leucine zipper structure. Biochemical and biophysical research communications. 1992; 187(1):375–380. [PubMed: 1520323]
39. Lin P, Le-Niculescu H, Hofmeister R, McCaffery JM, Jin M, Hennemann H, McQuistan T, De Vries L, Farquhar MG. The mammalian calcium-binding protein, nucleobindin (CALNUC), is a Golgi resident protein. The Journal of cell biology. 1998; 141(7):1515–1527. [PubMed: 9647645]
40. Longtine MS, McKenzie A 3rd, Demarini DJ, Shah NG, Wach A, Brachat A, Philippsen P, Pringle JR. Additional modules for versatile and economical PCR-based gene deletion and modification in Saccharomyces cerevisiae. Yeast (Chichester, England). 1998; 14(10):953–961.
41. Barlowe C. Coupled ER to Golgi transport reconstituted with purified cytosolic proteins. The Journal of cell biology. 1997; 139(5):1097–1108. [PubMed: 9382859]

42. Cao X, Ballew N, Barlowe C. Initial docking of ER-derived vesicles requires Uso1p and Ypt1p but is independent of SNARE proteins. The EMBO journal. 1998; 17(8):2156–2165. [PubMed: 9545229]
43. Sato K, Nakano A. Oligomerization of a cargo receptor directs protein sorting into COPII-coated transport vesicles. Molecular biology of the cell. 2003; 14(7):3055–3063. [PubMed: 12857885]
44. Schindler R, Itin C, Zerial M, Lottspeich F, Hauri HP. ERGIC-53, a membrane protein of the ER-Golgi intermediate compartment, carries an ER retention motif. European journal of cell biology. 1993; 61(1):1–9. [PubMed: 8223692]
45. Moussalli M, Pipe SW, Hauri HP, Nichols WC, Ginsburg D, Kaufman RJ. Mannose-dependent endoplasmic reticulum (ER)-Golgi intermediate compartment-53-mediated ER to Golgi trafficking of coagulation factors V and VIII. The Journal of biological chemistry. 1999; 274(46):32539–32542. [PubMed: 10551804]
46. Zhang B, Cunningham MA, Nichols WC, Bernat JA, Seligsohn U, Pipe SW, McVey JH, Schulte-Overberg U, de Bosch NB, Ruiz-Saez A, White GC, Tuddenham EG, Kaufman RJ, Ginsburg D. Bleeding due to disruption of a cargo-specific ER-to-Golgi transport complex. Nature genetics. 2003; 34(2):220–225. [PubMed: 12717434]
47. Nyfeler B, Zhang B, Ginsburg D, Kaufman RJ, Hauri HP. Cargo selectivity of the ERGIC-53/MCFD2 transport receptor complex. Traffic (Copenhagen, Denmark). 2006; 7(11):1473–1481.
48. Semenza JC, Hardwick KG, Dean N, Pelham HR. ERD2, a yeast gene required for the receptor-mediated retrieval of luminal ER proteins from the secretory pathway. Cell. 1990; 61(7):1349–1357. [PubMed: 2194670]
49. Ammerer G, Hunter CP, Rothman JH, Saari GC, Valls LA, Stevens TH. PEP4 gene of Saccharomyces cerevisiae encodes proteinase A, a vacuolar enzyme required for processing of vacuolar precursors. Molecular and cellular biology. 1986; 6(7):2490–2499. [PubMed: 3023936]
50. Schroder-Kohne S, Letourneur F, Riezman H. Alpha-COP can discriminate between distinct, functional di-lysine signals in vitro and regulates access into retrograde transport. Journal of cell science. 1998; 111(Pt 23):3459–3470. [PubMed: 9811561]
51. Stark C, Breitkreutz BJ, Reguly T, Boucher L, Breitkreutz A, Tyers M. BioGRID: a general repository for interaction datasets. Nucleic acids research. 2006; 34(Database issue):D535–D539. [PubMed: 16381927]
52. Denic V, Quan EM, Weissman JS. A luminal surveillance complex that selects misfolded glycoproteins for ER-associated degradation. Cell. 2006; 126(2):349–359. [PubMed: 16873065]
53. Vembar SS, Jonikas MC, Hendershot LM, Weissman JS, Brodsky JL. J domain co-chaperone specificity defines the role of BiP during protein translocation. The Journal of biological chemistry. 2010; 285(29):22484–22494. [PubMed: 20430885]
54. Travers KJ, Patil CK, Wodicka L, Lockhart DJ, Weissman JS, Walter P. Functional and genomic analyses reveal an essential coordination between the unfolded protein response and ER-associated degradation. Cell. 2000; 101(3):249–258. [PubMed: 10847680]
55. Schuldiner M, Collins SR, Thompson NJ, Denic V, Bhamidipati A, Punna T, Ihmels J, Andrews B, Boone C, Greenblatt JF, Weissman JS, Krogan NJ. Exploration of the function and organization of the yeast early secretory pathway through an epistatic miniarray profile. Cell. 2005; 123(3):507–519. [PubMed: 16269340]
56. Silberstein S, Schlenstedt G, Silver PA, Gilmore R. A role for the DnaJ homologue Scj1p in protein folding in the yeast endoplasmic reticulum. The Journal of cell biology. 1998; 143(4):921–933. [PubMed: 9817751]
57. Jonikas MC, Collins SR, Denic V, Oh E, Quan EM, Schmid V, Weibezahn J, Schwappach B, Walter P, Weissman JS, Schuldiner M. Comprehensive characterization of genes required for protein folding in the endoplasmic reticulum. Science (New York, NY). 2009; 323(5922):1693–1697.
58. Cox JS, Shamu CE, Walter P. Transcriptional induction of genes encoding endoplasmic reticulum resident proteins requires a transmembrane protein kinase. Cell. 1993; 73(6):1197–1206. [PubMed: 8513503]

59. Caldwell SR, Hill KJ, Cooper AA. Degradation of endoplasmic reticulum (ER) quality control substrates requires transport between the ER and Golgi. The Journal of biological chemistry. 2001; 276(26):23296–23303. [PubMed: 11316816]
60. Vashist S, Kim W, Belden WJ, Spear ED, Barlowe C, Ng DT. Distinct retrieval and retention mechanisms are required for the quality control of endoplasmic reticulum protein folding. The Journal of cell biology. 2001; 155(3):355–368. [PubMed: 11673477]
61. Vashist S, Ng DT. Misfolded proteins are sorted by a sequential checkpoint mechanism of ER quality control. The Journal of cell biology. 2004; 165(1):41–52. [PubMed: 15078901]
62. Fujita M, Yoko OT, Jigami Y. Inositol deacylation by Bst1p is required for the quality control of glycosylphosphatidylinositol-anchored proteins. Molecular biology of the cell. 2006; 17(2):834–850. [PubMed: 16319176]
63. Kincaid MM, Cooper AA. Misfolded proteins traffic from the endoplasmic reticulum (ER) due to ER export signals. Molecular biology of the cell. 2007; 18(2):455–463. [PubMed: 17108324]
64. Dancourt J, Barlowe C. Erv26p–dependent export of alkaline phosphatase from the ER requires lumenal domain recognition. Traffic (Copenhagen, Denmark). 2009; 10(8):1006–1018.
65. Kamiya Y, Yamaguchi Y, Takahashi N, Arata Y, Kasai K, Ihara Y, Matsuo I, Ito Y, Yamamoto K, Kato K. Sugar-binding properties of VIP36, an intracellular animal lectin operating as a cargo receptor. The Journal of biological chemistry. 2005; 280(44):37178–37182. [PubMed: 16129679]
66. Nawa D, Shimada O, Kawasaki N, Matsumoto N, Yamamoto K. Stable interaction of the cargo receptor VIP36 with molecular chaperone BiP. Glycobiology. 2007; 17(9):913–921. [PubMed: 17586539]
67. Reiterer V, Nyfeler B, Hauri HP. Role of the lectin VIP36 in post-ER quality control of human alpha1-antitrypsin. Traffic (Copenhagen, Denmark). 2010; 11(8):1044–1055.
68. Spear ED, Ng DT. Stress tolerance of misfolded carboxypeptidase Y requires maintenance of protein trafficking and degradative pathways. Molecular biology of the cell. 2003; 14(7):2756–2767. [PubMed: 12857862]
69. Kawaguchi S, Hsu CL, Ng DT. Interplay of substrate retention and export signals in endoplasmic reticulum quality control. PloS one. 2010; 5(11):e15532. [PubMed: 21151492]
70. Finger A, Knop M, Wolf DH. Analysis of two mutated vacuolar proteins reveals a degradation pathway in the endoplasmic reticulum or a related compartment of yeast. European journal of biochemistry / FEBS. 1993; 218(2):565–574. [PubMed: 8269947]
71. Ng DT, Spear ED, Walter P. The unfolded protein response regulates multiple aspects of secretory and membrane protein biogenesis and endoplasmic reticulum quality control. The Journal of cell biology. 2000; 150(1):77–88. [PubMed: 10893258]
72. Tong AH, Boone C. Synthetic genetic array analysis in Saccharomyces cerevisiae. Methods in molecular biology (Clifton, NJ). 2006; 313:171–192.
73. Dhungel N, Eleuteri S, Li LB, Kramer NJ, Chartron JW, Spencer B, Kosberg K, Fields JA, Stafa K, Adame A, Lashuel H, Frydman J, Shen K, Masliah E, Gitler AD. Parkinson's disease genes VPS35 and EIF4G1 interact genetically and converge on alpha-synuclein. Neuron. 2015; 85(1): 76–87. [PubMed: 25533483]
74. Ram AF, Kapteyn JC, Montijn RC, Caro LH, Douwes JE, Baginsky W, Mazur P, van den Ende H, Klis FM. Loss of the plasma membrane-bound protein Gas1p in Saccharomyces cerevisiae results in the release of beta1,3-glucan into the medium and induces a compensation mechanism to ensure cell wall integrity. Journal of bacteriology. 1998; 180(6):1418–1424. [PubMed: 9515908]
75. Mouyna I, Fontaine T, Vai M, Monod M, Fonzi WA, Diaquin M, Popolo L, Hartland RP, Latge JP. Glycosylphosphatidylinositol-anchored glucanosyltransferases play an active role in the biosynthesis of the fungal cell wall. The Journal of biological chemistry. 2000; 275(20):14882–14889. [PubMed: 10809732]
76. Jungmann J, Rayner JC, Munro S. The Saccharomyces cerevisiae protein Mnn10p/Bed1p is a subunit of a Golgi mannosyltransferase complex. The Journal of biological chemistry. 1999; 274(10):6579–6585. [PubMed: 10037752]
77. Orlean P. Architecture and biosynthesis of the Saccharomyces cerevisiae cell wall. Genetics. 2012; 192(3):775–818. [PubMed: 23135325]

78. Arias P, Diez-Muniz S, Garcia R, Nombela C, Rodriguez-Pena JM, Arroyo J. Genome-wide survey of yeast mutations leading to activation of the yeast cell integrity MAPK pathway: novel insights into diverse MAPK outcomes. BMC genomics. 2011; 12:390. [PubMed: 21810245]

79. Levin DE. Regulation of cell wall biogenesis in Saccharomyces cerevisiae: the cell wall integrity signaling pathway. Genetics. 2011; 189(4):1145–1175. [PubMed: 22174182]

80. Scrimale T, Didone L, de Mesy Bentley KL, Krysan DJ. The unfolded protein response is induced by the cell wall integrity mitogen-activated protein kinase signaling cascade and is required for cell wall integrity in Saccharomyces cerevisiae. Molecular biology of the cell. 2009; 20(1):164–175. [PubMed: 18971375]

81. Chen Y, Feldman DE, Deng C, Brown JA, De Giacomo AF, Gaw AF, Shi G, Le QT, Brown JM, Koong AC. Identification of mitogen-activated protein kinase signaling pathways that confer resistance to endoplasmic reticulum stress in Saccharomyces cerevisiae. Molecular cancer research : MCR. 2005; 3(12):669–677. [PubMed: 16380504]

82. Babour A, Bicknell AA, Tourtellotte J, Niwa M. A surveillance pathway monitors the fitness of the endoplasmic reticulum to control its inheritance. Cell. 2010; 142(2):256–269. [PubMed: 20619447]

83. Velloso LM, Svensson K, Pettersson RF, Lindqvist Y. The crystal structure of the carbohydrate-recognition domain of the glycoprotein sorting receptor p58/ERGIC-53 reveals an unpredicted metal-binding site and conformational changes associated with calcium ion binding. Journal of molecular biology. 2003; 334(5):845–851. [PubMed: 14643651]

84. Weis WI, Drickamer K. Structural basis of lectin-carbohydrate recognition. Annual review of biochemistry. 1996; 65:441–473.

85. Appenzeller-Herzog C, Roche AC, Nufer O, Hauri HP. pH-induced conversion of the transport lectin ERGIC-53 triggers glycoprotein release. The Journal of biological chemistry. 2004; 279(13):12943–12950. [PubMed: 14718532]

86. Kamiya Y, Kamiya D, Yamamoto K, Nyfeler B, Hauri HP, Kato K. Molecular basis of sugar recognition by the human L-type lectins ERGIC-53, VIPL, and VIP36. The Journal of biological chemistry. 2008; 283(4):1857–1861. [PubMed: 18025080]

87. Niphakis MJ, Lum KM, Cognetta AB 3rd, Correia BE, Ichu TA, Olucha J, Brown SJ, Kundu S, Piscitelli F, Rosen H, Cravatt BF. A Global Map of Lipid-Binding Proteins and Their Ligandability in Cells. Cell. 2015; 161(7):1668–1680. [PubMed: 26091042]

88. Zhang B. Recent developments in the understanding of the combined deficiency of FV and FVIII. British journal of haematology. 2009; 145(1):15–23. [PubMed: 19183188]

89. Nishio M, Kamiya Y, Mizushima T, Wakatsuki S, Sasakawa H, Yamamoto K, Uchiyama S, Noda M, McKay AR, Fukui K, Hauri HP, Kato K. Structural basis for the cooperative interplay between the two causative gene products of combined factor V and factor VIII deficiency. Proceedings of the National Academy of Sciences of the United States of America. 2010; 107(9):4034–4039. [PubMed: 20142513]

90. Satoh T, Suzuki K, Yamaguchi T, Kato K. Structural basis for disparate sugar-binding specificities in the homologous cargo receptors ERGIC-53 and VIP36. PloS one. 2014; 9(2):e87963. [PubMed: 24498414]

91. Kawasaki N, Ichikawa Y, Matsuo I, Totani K, Matsumoto N, Ito Y, Yamamoto K. The sugar-binding ability of ERGIC-53 is enhanced by its interaction with MCFD2. Blood. 2008; 111(4): 1972–1979. [PubMed: 18056485]

92. Zheng C, Page RC, Das V, Nix JC, Wigren E, Misra S, Zhang B. Structural characterization of carbohydrate binding by LMAN1 protein provides new insight into the endoplasmic reticulum export of factors V (FV) and VIII (FVIII). The Journal of biological chemistry. 2013; 288(28): 20499–20509. [PubMed: 23709226]

93. Sherman F. Getting started with yeast. Methods in enzymology. 1991; 194:3–21. [PubMed: 2005794]

94. Gietz RD, Schiestl RH. High-efficiency yeast transformation using the LiAc/SS carrier DNA/PEG method. Nature protocols. 2007; 2(1):31–34. [PubMed: 17401334]

95. Rossanese OW, Reinke CA, Bevis BJ, Hammond AT, Sears IB, O'Connor J, Glick BS. A role for actin, Cdc1p, and Myo2p in the inheritance of late Golgi elements in Saccharomyces cerevisiae. The Journal of cell biology. 2001; 153(1):47–62. [PubMed: 11285273]

96. Rothman JH, Stevens TH. Protein sorting in yeast: mutants defective in vacuole biogenesis mislocalize vacuolar proteins into the late secretory pathway. Cell. 1986; 47(6):1041–1051. [PubMed: 3536126]

97. Sikorski RS, Hieter P. A system of shuttle vectors and yeast host strains designed for efficient manipulation of DNA in Saccharomyces cerevisiae. Genetics. 1989; 122(1):19–27. [PubMed: 2659436]

98. Christianson TW, Sikorski RS, Dante M, Shero JH, Hieter P. Multifunctional yeast high-copy-number shuttle vectors. Gene. 1992; 110(1):119–122. [PubMed: 1544568]

99. Prinz WA, Grzyb L, Veenhuis M, Kahana JA, Silver PA, Rapoport TA. Mutants affecting the structure of the cortical endoplasmic reticulum in Saccharomyces cerevisiae. The Journal of cell biology. 2000; 150(3):461–474. [PubMed: 10931860]

100. Stirling CJ, Rothblatt J, Hosobuchi M, Deshaies R, Schekman R. Protein translocation mutants defective in the insertion of integral membrane proteins into the endoplasmic reticulum. Molecular biology of the cell. 1992; 3(2):129–142. [PubMed: 1550957]

101. Rothblatt JA, Deshaies RJ, Sanders SL, Daum G, Schekman R. Multiple genes are required for proper insertion of secretory proteins into the endoplasmic reticulum in yeast. The Journal of cell biology. 1989; 109(6 Pt 1):2641–2652. [PubMed: 2687285]

102. Fankhauser C, Conzelmann A. Purification, biosynthesis and cellular localization of a major 125-kDa glycophosphatidylinositol-anchored membrane glycoprotein of Saccharomyces cerevisiae. European journal of biochemistry / FEBS. 1991; 195(2):439–448. [PubMed: 1847682]

103. Wilson JD, Barlowe C. Yet1p and Yet3p, the yeast homologs of BAP29 and BAP31, interact with the endoplasmic reticulum translocation apparatus and are required for inositol prototrophy. The Journal of biological chemistry. 2010; 285(24):18252–18261. [PubMed: 20378542]

104. Decottignies A, Evain A, Ghislain M. Binding of Cdc48p to a ubiquitin-related UBX domain from novel yeast proteins involved in intracellular proteolysis and sporulation. Yeast (Chichester, England). 2004; 21(2):127–139.

105. Barlowe C, d'Enfert C, Schekman R. Purification and characterization of SAR1p, a small GTP-binding protein required for transport vesicle formation from the endoplasmic reticulum. The Journal of biological chemistry. 1993; 268(2):873–879. [PubMed: 8419365]

106. Brodsky JL, Hamamoto S, Feldheim D, Schekman R. Reconstitution of protein translocation from solubilized yeast membranes reveals topologically distinct roles for BiP and cytosolic Hsc70. The Journal of cell biology. 1993; 120(1):95–102. [PubMed: 8416998]

107. Meusser B, Sommer T. Vpu-mediated degradation of CD4 reconstituted in yeast reveals mechanistic differences to cellular ER-associated protein degradation. Molecular cell. 2004; 14(2):247–258. [PubMed: 15099523]

108. Collins SR, Schuldiner M, Krogan NJ, Weissman JS. A strategy for extracting and analyzing large-scale quantitative epistatic interaction data. Genome biology. 2006; 7(7):R63. [PubMed: 16859555]

109. Boyle EI, Weng S, Gollub J, Jin H, Botstein D, Cherry JM, Sherlock G. GO::TermFinder--open source software for accessing Gene Ontology information and finding significantly enriched Gene Ontology terms associated with a list of genes. Bioinformatics (Oxford, England). 2004; 20(18):3710–3715.

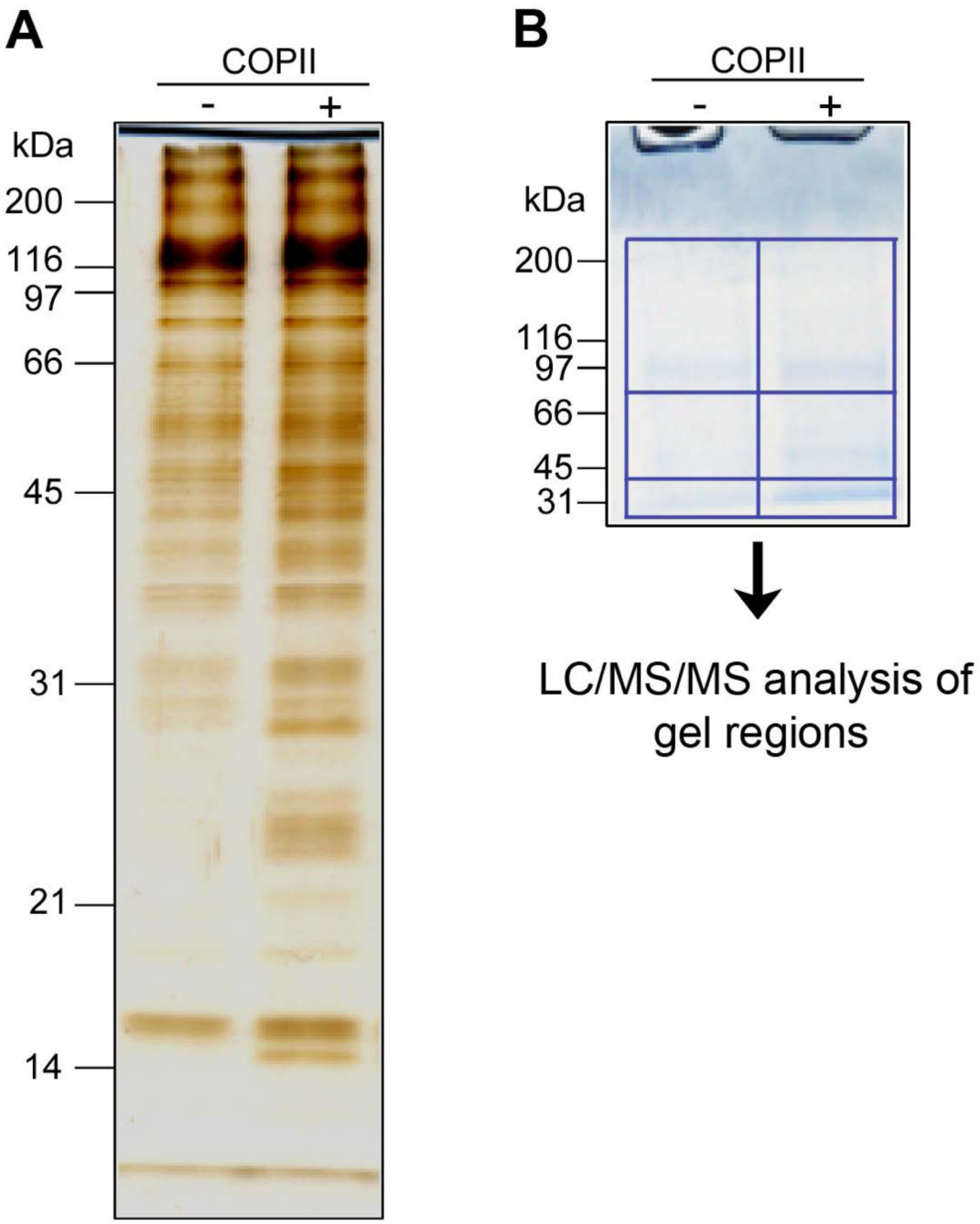

Figure 1. Preparation of COPII vesicles for analysis by mass spectrometry

A) Nycodenz gradient isolated COPII vesicles visualized by silver stain. B) Vesicles as in (A) run partially (~1.7 cm) into an SDS-PAGE gel and visualized with colloidal Coomassie. Rectangles denote the partitions of the gel submitted for peptide identification by mass spectrometry.

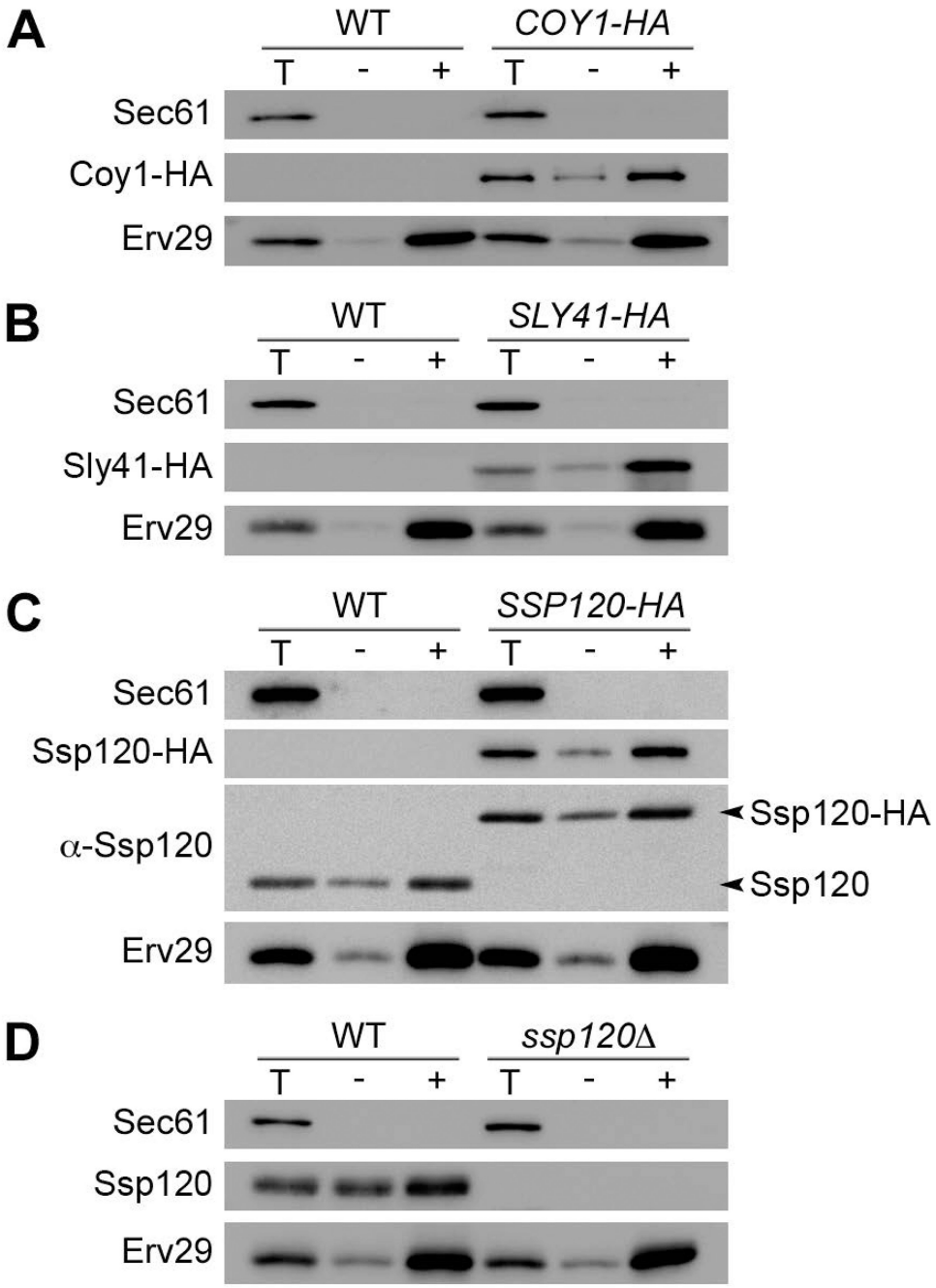

Figure 2. Efficient packaging of ER-vesicle proteins into COPII-coated vesicles

(A–C) *In vitro* budding assays with semi-intact cells prepared from wild-type (BY4742) cells and strains expressing Coy1-HA (A), Sly41-HA (B), or Ssp120-HA (C). One-tenth of a total reaction (T) was compared to budded vesicles produced in the absence (−) or presence (+) of COPII proteins. Tagged proteins were visualized by immunoblot with anti-HA antibody, and Sec61 (ER resident) as a negative control and Erv29 (COPII vesicle protein) as a positive control were detected using polyclonal antisera. Samples from (C) were resolved on a parallel SDS-PAGE gel and immunoblotted with anti-Ssp120 polyclonal

antibody (blot labeled α-Ssp120). The HA-tagged and native forms of Ssp120 are indicated. D) *In vitro* budding assay with microsomes prepared from wild-type (BY4742) and *ssp120*Δ strains performed as in (A–C). Proteins were detected by immunoblot with polyclonal antisera against Sec61, Ssp120, and Erv29.

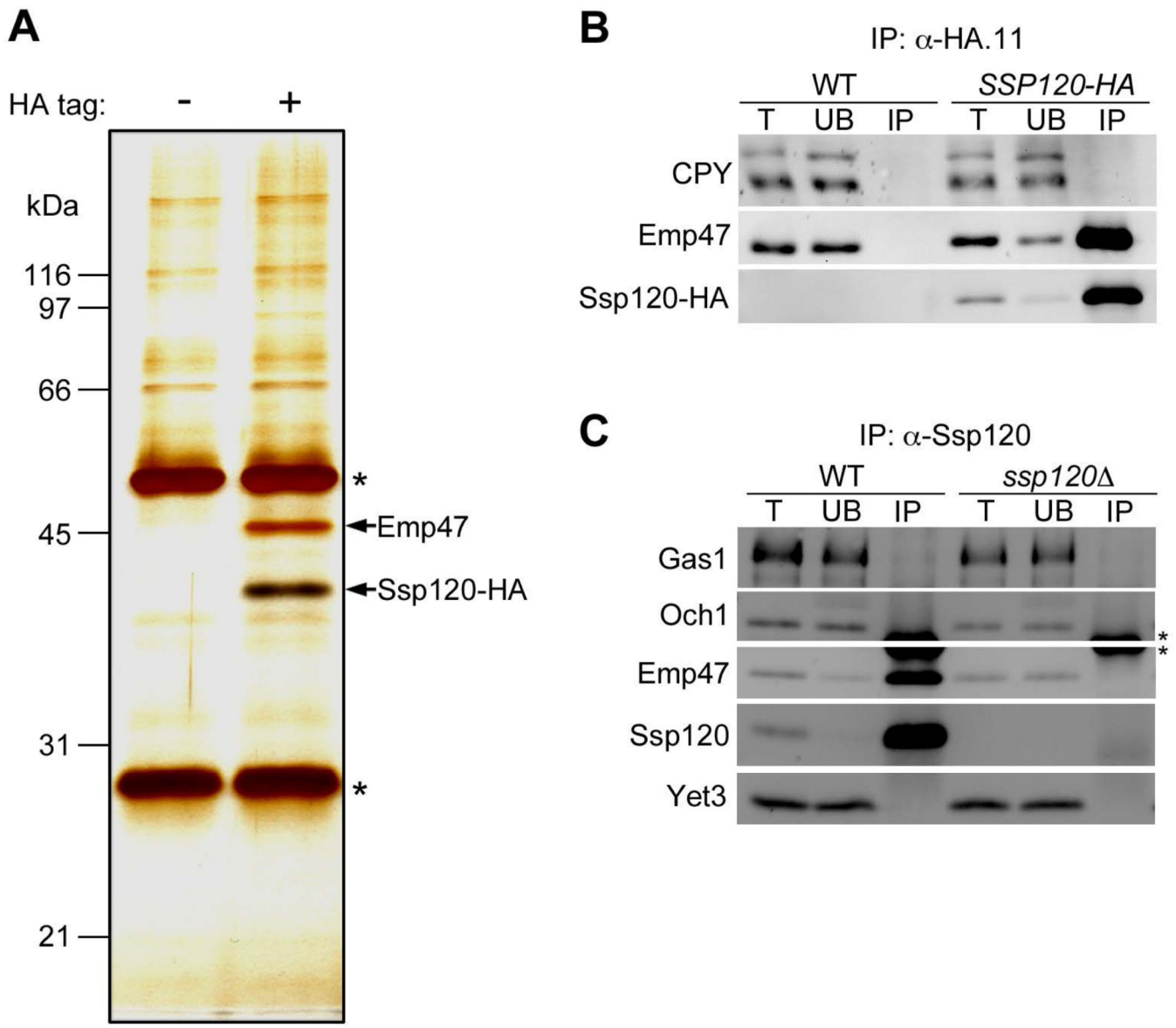

Figure 3. Emp47 co-immunoprecipitates with Ssp120-HA

A) Budding-competent microsomes prepared from untagged (BY4742) and *SSP120-HA* strains were solubilized in Triton X-100 and subjected to immunoprecipitation with anti-HA monoclonal antibodies. After washing, immunoprecipitated complexes were denatured in SDS-containing sample buffer, resolved on an SDS-PAGE gel, and visualized by silver stain. Arrows indicate bands that were excised (from a parallel colloidal Coomassie-stained gel, not shown) and identified by mass spectrometry. Asterisks indicate the position of anti-HA antibody heavy and light chains. B) Immunoprecipitations performed as in (A) comparing total input (T), unbound (UB), and IP samples. Proteins were detected by immunoblot with anti-HA antibodies (for Ssp120-HA) or polyclonal antisera against Emp47 and CPY (negative control). C) Triton X-100 solubilized microsomes from wild-type (BY4742) and *ssp120*Δ strains were immunoprecipitated with anti-Ssp120 polyclonal

antiserum and analyzed as in (B). Gas1, Och1, and Yet3 were included as negative controls. Asterisk indicates anti-Ssp120 heavy chain.

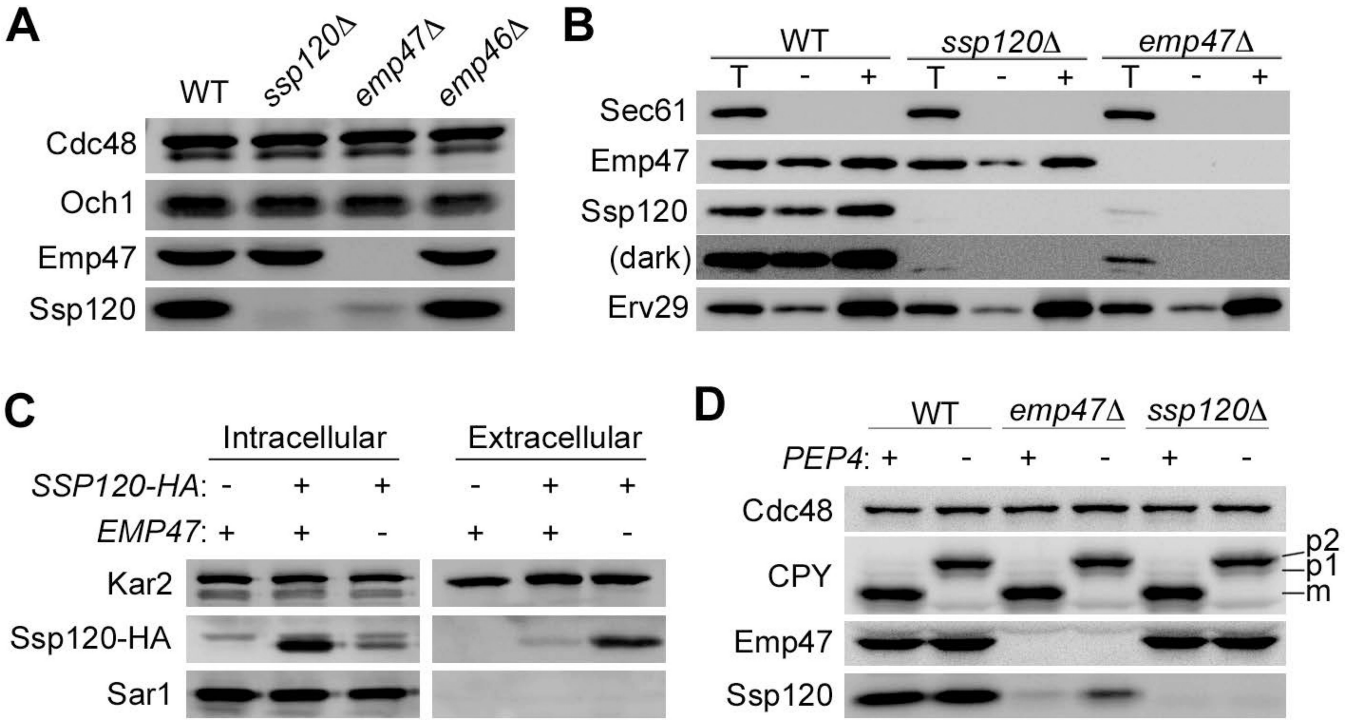

Figure 4. Ssp120 requires Emp47 for proper localization

A) Immunoblot analysis of the steady-state levels of Ssp120 and Emp47 in wild-type (BY4742), *ssp120*Δ, *emp47*Δ, and *emp46*Δ strains. Whole-cell lysates were prepared as described in Materials and Methods, and equal amounts resolved on an SDS-PAGE gel. Proteins were detected with polyclonal anti-sera against Cdc48 (control), Och1 (control), Emp47, and Ssp120. B) *In vitro* budding assay with microsomes prepared from wild-type (BY4742), *ssp120*Δ, and *emp47*Δ strains performed as described in the legend of Figure 2A. Proteins were detected with polyclonal anti-sera against Emp47, Sec61 (negative control), Ssp120, and Erv29 (positive control). The panel labeled '(dark)' shows a saturated exposure of the anti-Ssp120 blot to visualize the low levels of protein in the *emp47*Δ background. C) Amount of Ssp120-HA secreted after 6 hr in wild-type (BY4742), *SSP120-HA*, and *emp47*Δ *SSP120-HA* strains was detected by immunoblotting whole cell lysates ("Intracellular") and TCA-precipitated culture medium ("Extracellular") with anti-HA antibody for Ssp120-HA and polyclonal antisera against Kar2 as a positive control and Sar1 as a negative control. D) Immunoblot analysis of the influence of a *PEP4* deletion on steady-state levels of Ssp120 and Emp47 in wild-type (BY4742), *emp47*Δ, and *ssp120*Δ strains performed as in (A). Proteins were detected with polyclonal anti-sera against Cdc48 (loading control), CPY (control for *pep4*Δ), Emp47, and Ssp120. The ER (p1), Golgi (p2), and mature (m) forms of CPY are indicated.

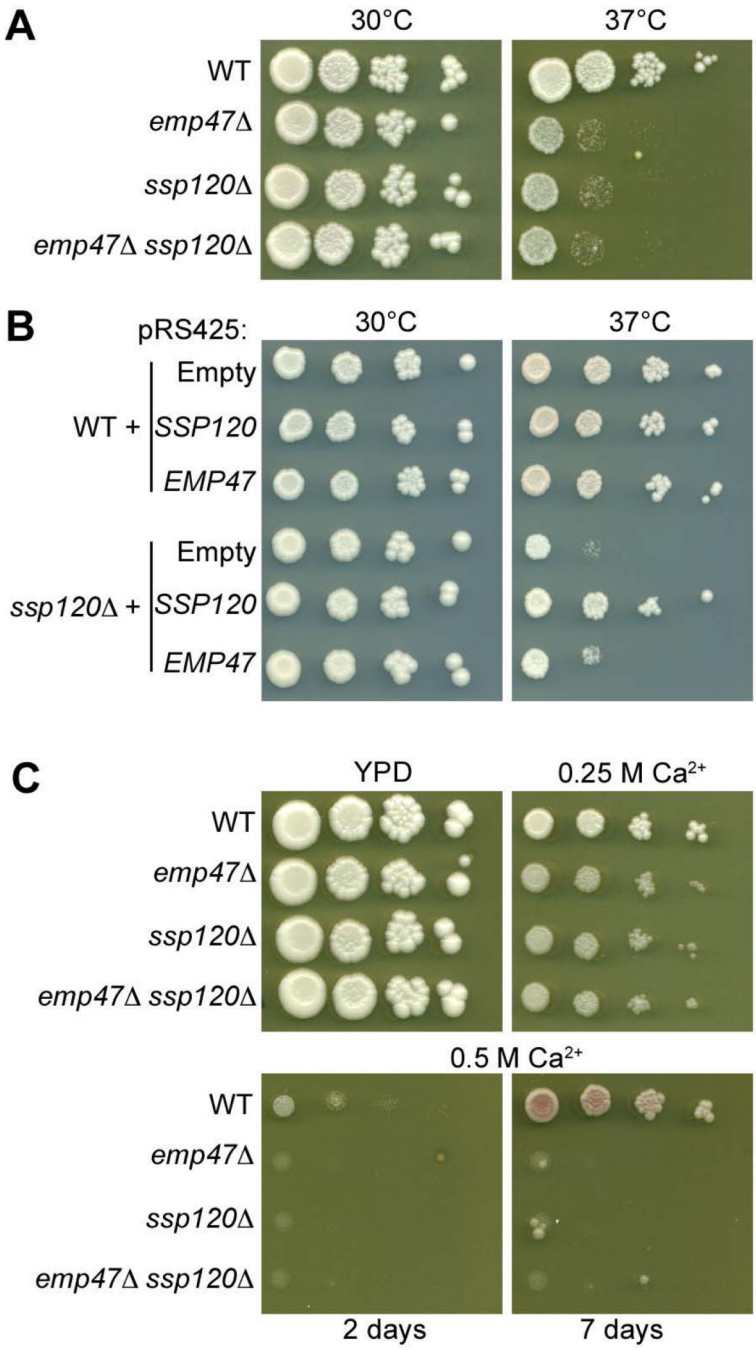

Figure 5. Growth comparison of *ssp120*Δ and *emp47*Δ strains

A) Temperature sensitivity of the *emp47*Δ and *ssp120*Δ strains. Wild-type (W303a), *emp47*Δ, *ssp120*Δ, and *emp47*Δ *ssp120*Δ strains were grown to saturation in YPD at 30°C and adjusted to an OD_{600} of 1.0. A 10-fold dilution series was spotted onto YPD and incubated at the indicated temperatures for 2 days. B) Overexpression of Emp47 does not suppress the temperature sensitivity of the *ssp120*Δ strain. Wild-type (W303a) and *ssp120*Δ strains carrying empty vector (pRS425) or multicopy *EMP47* or *SSP120* (pNM23 or pNM17) expression plasmids were grown to saturation in SC-Leu at 30°C and adjusted to an

OD_{600} of 1.0. A 10-fold dilution series was spotted onto SC-Leu and incubated at the indicated temperatures for 3 days. C) Calcium sensitivity of the *emp47*Δ and *ssp120*Δ strains. Wild-type (W303a), *emp47*Δ, *ssp120*Δ, and *emp47*Δ *ssp120*Δ strains were prepared as in (A) and spotted onto YPD or YPD containing 0.25 M or 0.5 M $CaCl_2$ and incubated for 2 days at 30°C. Incubation of the 0.5M $CaCl_2$ plate was extended to 7 days to rule out masking effects from slow growth (bottom right panel).

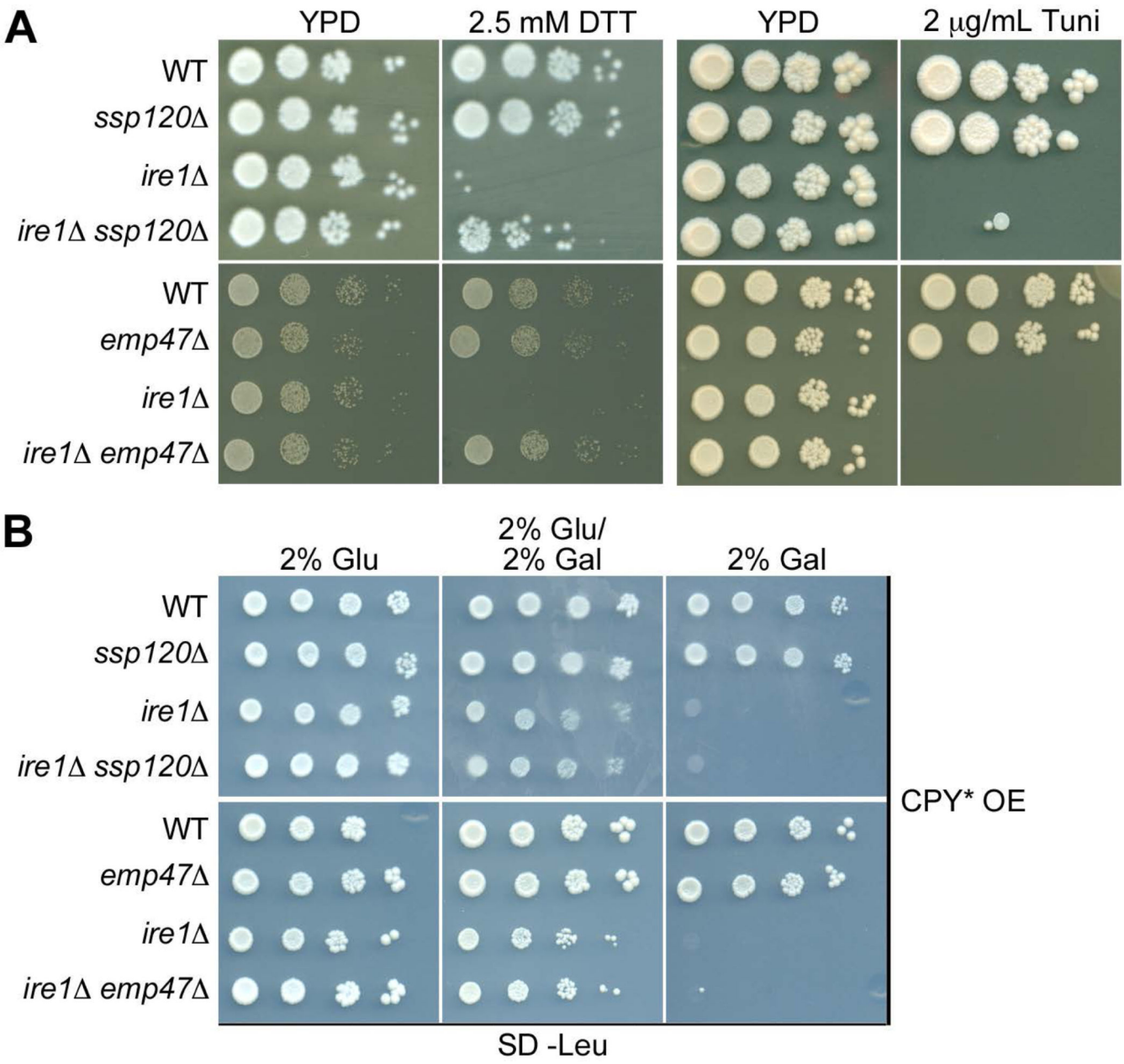

Figure 6. Effects of *ssp120*Δ and *emp47*Δ mutations on *ire1*Δ cell growth under UPR-inducing conditions

A) *SSP120* and *EMP47* deletions suppress sensitivity of *ire1*Δ cells to DTT, but not tunicamycin. Wild-type (BY4742), *ssp120*Δ, *ire1*Δ, *ssp120*Δ *ire1*Δ, *emp47*Δ, *and emp47*Δ *ire1*Δ strains were prepared as described in Figure 5A and grown at 30°C on YPD, YPD with 2.5 mM DTT for 1 day (left panels) or YPD with 2 μg/mL tunicamycin for 2 days (right panels). The experiments with the *ssp120*Δ strain set (top panels) and *emp47*Δ strain set (bottom panels) were conducted on separated occasions. B) *SSP120* and *EMP47* deletions do not suppress sensitivity of *ire1*Δ cells to overexpression of CPY*. Wild-type (BY4742), *ssp120*Δ, *ire1*Δ, *ssp120*Δ *ire1*Δ, *emp47*Δ, *and emp47*Δ *ire1*Δ strains carrying a plasmid with *CPY** under control of the *GAL1* promoter (pES28) were prepared as described

in Materials and Methods and a 10-fold dilution series plated onto selective medium with 2% glucose (no expression), 2% galactose (overexpression), or a mixture (attenuated expression) and grown at 30°C for 4 days.

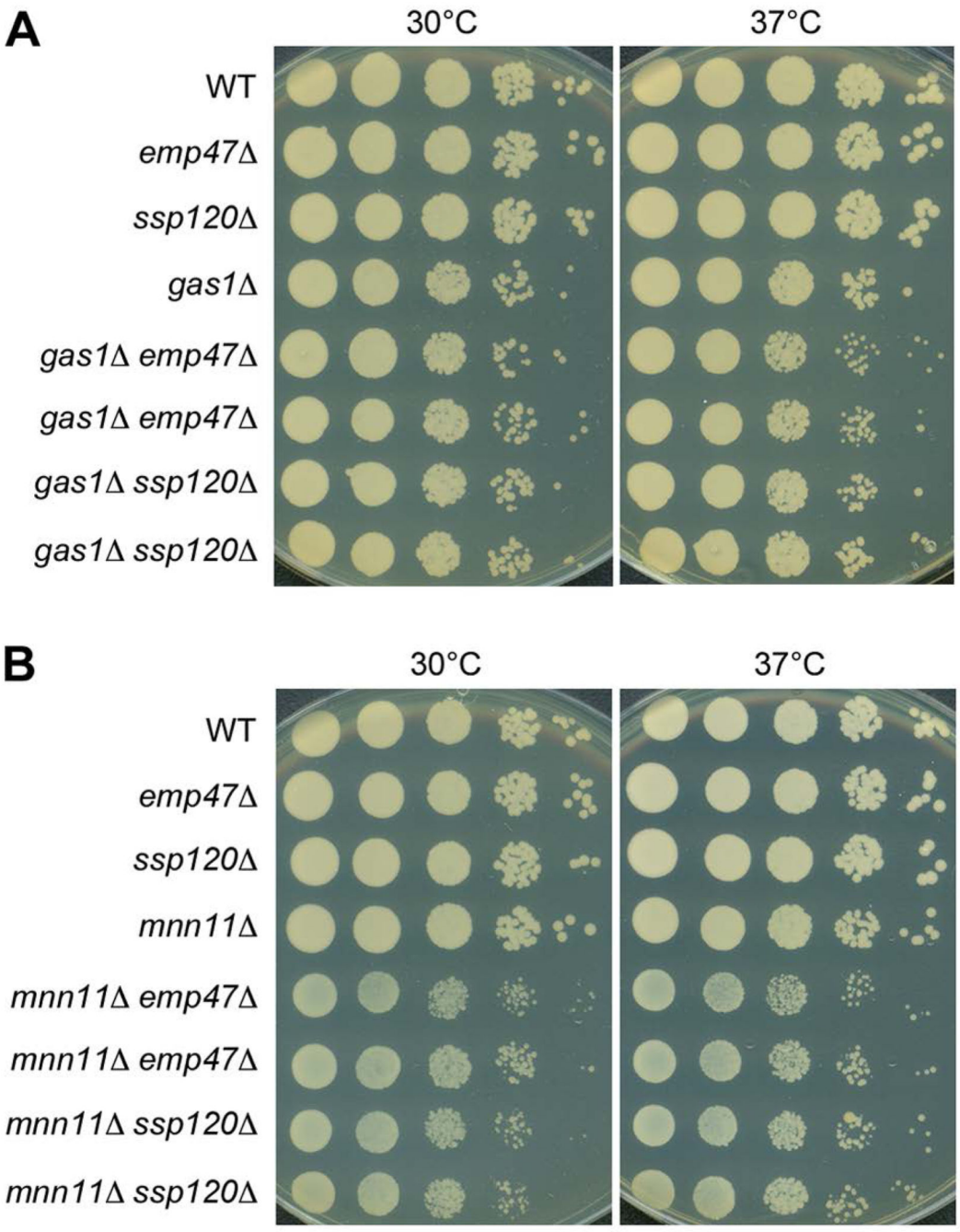

Figure 7. *EMP47* and *SSP120* display synthetic negative interaction with GAS1 and MNN11

A) A 10-fold dilution series of wild-type (BY4742), *emp47*Δ, *ssp120*Δ, *gas1*Δ, *gas1*Δ *emp47*Δ (2 independent isolates), *and gas1*Δ *ssp120*Δ (2 independent isolates) cells were spotted onto YPD plates and grown at 30°C and 37°C for 2 days. B) Similarly, wild-type (BY4742), *emp47*Δ, *ssp120*Δ, *mnn11*Δ, *mnn11*Δ *emp47*Δ (2 independent isolates), *and mnn11*Δ *ssp120*Δ (2 independent isolates) cells were spotted onto YPD plates and grown at 30°C and 37°C for 2 days.

Table 1

Peptide representation of various classes of ER vesicle proteins

ORF	Protein	Unique peptides		Description
		−COPII	+ COPII	
***Erv proteins reported in Otte et al., 2001* (19)**				
YIL004C	Bet1	0	2	ER and Golgi Qc-SNARE protein
YGL200C	Emp24	0	5	Member of the p24 family involved in ER to Golgi transport
YFL048C	Emp47	5	9	Type I membrane protein of ER-derived COPII-coated vesicles
YAR002C–A	Erp1	3	5	Member of the p24 family involved in ER to Golgi transport
YAL007C	Erp2	1	4	Member of the p24 family involved in ER to Golgi transport
YGL054C	Erv14	1	3	Protein localized to COPII-coated vesicles, cargo receptor
YML012W	Erv25	1	7	Member of the p24 family involved in ER to Golgi transport
YGR284C	Erv29	2	11	Protein localized to COPII-coated vesicles, cargo receptor
YML067C	Erv41	0	13	Protein localized to COPII-coated vesicles, involved in retention
YAL042W	Erv46	0	5	Protein localized to COPII-coated vesicles, involved in retention
YCL001W	Rer1	1	6	Protein involved in retention of membrane proteins
YNL263C	Yif1	0	4	Integral membrane protein, Yip1 interacting factor
YNL044W	Yip3	0	0	Protein localized to COPII vesicles
ER vesicle proteins in other reports (19, 27–29, 31)				
YEL036C	Anp1	1	1	Subunit of Golgi mannosyltransferase complex
YLR078C	Bos1	0	4	ER and Golgi Qb-SNARE protein
YBL040C	Erd2	0	5	HDEL receptor, retrieves ER resident proteins
YHR181W	Erv26	1	7	Integral membrane protein of the early Golgi apparatus and ER
YBR205W	Ktr3	0	6	Golgi-localized mannosyltransferase
YPL050C	Mnn9	3	5	Subunit of Golgi mannosyltransfease complex
YGL038C	Och1	0	3	Golgi-localized outer chain mannosyltransferase
YLR268W	Sec22	0	2	ER and Golgi R-SNARE protein
YLR026C	Sed5	1	5	cis-Golgi Qa-SNARE protein, syntaxin family
YGR172C	Yip1	0	1	Integral membrane protein
New proteins with ER vesicle-like peptide representation				
YKL179C	Coy1	0	7	Golgi membrane protein with similarity to mammalian CASP
YOR307C	Sly41	0	4	Protein involved in ER-to-Golgi transport
YLR250W	Ssp120	4	8	Protein of unknown function
Secretory cargo detected in ER vesicles				
YDR058W	Fet3	0	3	Plasma membrane ferro-oxidoreductase, involved in iron uptake
YMR307W	Gas1	1	5	Plasma membrane GPI-anchored β-glucanosyltransferase
YDR345C	Hxt3	4	7	Plasma membrane glucose transporter
YDR245W	Mnn10	0	3	Subunit of a Golgi mannosyltransferase complex
YOR153W	Pdr5	0	10	Plasma membrane ATP-binding cassette (ABC) transporter
YGL008C	Pma1	21	30	Plasma membrane H+-ATPase
YOR270C	Vph1	7	22	Subunit a of vacuolar-ATPase V0 domain
YJL012C	Vtc4	5	20	Vacuolar membrane polyphosphate polymerase

ORF	Protein	Unique peptides		Description
		−COPII	+ COPII	
YDR135C	Ycf1	0	11	Vacuolar glutathione S-conjugate transporter